Delay Analysis of Molecular Communication Using Filaments and Relay-Enabled Nodes

By:
Kamaloddin
Darchinimaragheh

A Thesis submitted to the Faculty of Graduate Studies of
The University of Manitoba
in partial fulfilment of the requirements of the degree of
Doctor of Philosophy

Department of Electrical and Computer Engineering
University of Manitoba
Winnipeg

Abstract

In this thesis, we suggest using nano-relays in a network using molecular communication in free space to improve the performance of the system in terms of delay. An approximation method for jump diffusion processes, which is based on Markov chains, is used to model molecular propagation in such scenarios. The model is validated through comparing analytic results with simulation results. The results illustrate the advantage of using nano-relays over diffusion in terms of delay. The proposed model is then used to investigate the effect of different parameters, such as filaments' length and the number of filaments attached to each nano-relay, on the delay performance of the communication technique.

We used transient solution of the model in the first set of results. However, stationary solution of the model can generate useful results, too. In the second set of results, the model is extended for an unbounded scenario. Considering the propagation as a one-sided skip free process and using matrix analytic methods, we find the final distribution for the position of information molecules. It will be shown that it is possible to keep molecules in a desired region. The effect of different parameters on the final distribution for the position of information molecules is investigated, too. This analysis can be useful in drug delivery applications.

Acknowledgment

I want to express my deep thanks to my advisor, Professor A. S. Alfa; for his encouragement, support and thoughtful guidance. I also want to thank other professors in my PhD committee: Dr. Jun Cai, Dr. Rasit Eskicioglu, Dr. Azzedine Boukerche, and Dr. Jeff Diamond. Finally, I want to express my gratitude to Dr. Elisavet Kardami and Dr. Stephanie Portet for their help and advice regarding biological issues of my research.

Contents

List of Figures

Chapter 1

Introduction

The concept of manipulating materials at molecular level was first pointed out in Richard Feynman's speech "There Is Plenty of Room at the Bottom" in 1959. Since then, there have been huge advancements in the field and now it is recognized as nano-technology. Recent achievements in nanotechnology promise our ability to build functional units capable of performing simple tasks at molecular level. At this scale, we call these units nano-machines. Figure 1.1 shows an illustration of a nano-machine.

Interconnection of nano-machines constitutes nano-networks. Nano-networks provide means for cooperation and information sharing among nano-machines, allowing them to fulfill more complex tasks. Considering the size of nano-machines, nano-networks could carry out complex tasks in different applications like: bio-medical applications (immune system support, bio-hybrid implants, drug delivery systems, health monitoring, and genetic engineering),

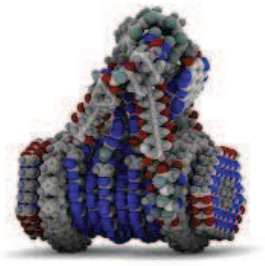

Figure 1.1: Nano-machine is a molecular level entity [1].

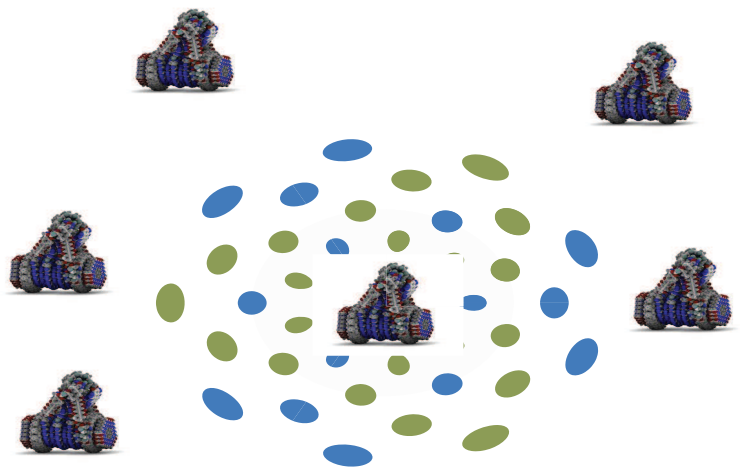

Figure 1.2: A sample nano-network.

industrial and consumer goods applications (food and water quality control), military applications (nuclear, biological, and chemical defense, nano-functionalized equipment), and environmental applications (bio-degradation, air pollution control) [4]. Figure 1.2 represents a sample nano-network in which, the nano-machine in the middle is transmitting a message using blue and green molecules to the nano-machines around it.

In order to make the cooperation among nano-machines happen, communication methods should be used in nano-networks. Communication in a nano-network can be categorized, with respect to the type of nodes participating in it, as follows:

- Communication between nano-machines and larger systems such as electronic micro-devices, and
- Communication between two or more nano-machines.

In this thesis, we focus on communication between two or more nano-machines.

In classical wireless communication networks, electromagnetic waves in megahertz frequency bands are used to transmit data from a transmitter to the receiver. To establish a wireless communication with classical approaches in nano-networks, nano-machines should be integrated with radio frequency transceivers and nano-scale antennas. However, due to the size and complexity issues, transceivers cannot be integrated into nano-machines easily.

In addition, if it were possible, enough power output of the transceiver would be another issue [4].

There are four major approaches proposed to be used in nano-networks for communications: terahertz electromagnetic communication, quantum communication, communication with fluorescence resonance energy transfer, and molecular communication [4]. In terahertz electromagnetic communication, electromagnetic waves in terahertz frequency bands are used to transmit data. Using these frequency bands makes it possible to build efficient transceivers in molecular scales. Carbon nano-tubes are one of the top candidate materials to be used in the transceivers, because they exhibit unique electrical properties which result in an efficient performance in terms of power consumption, robustness, etc. [5]. Quantum communication is the process of transferring quantum states from a transmitter to the receiver. The most common method to do so is quantum teleportation. Quantum teleportation is the process of sending quantum states using entangled (entanglement occurs when particles interact physically and then become separated) qubits (the basic unit of quantum information) [6]. Fluorescence resonance energy transfer is the process of energy transfer between two chromophores (a chromophore is the part of a molecule responsible for its color). This energy transfer is carried out through a dipole-dipole coupling. Communication with fluorescence resonance energy transfer uses this energy transfer to transmit data [7]. Molecular communication is a bio-inspired solution. There are already many molecular scale machines in nature, such as cells of human body, communicating with each other. Inspired by them, molecular communication is defined as the process in which information is encoded in molecules. Transceivers are nano-machines which are capable of releasing specific types of molecules as a response to an external or internal command, or reacting appropriately upon receiving different types of molecules [4]. In this thesis, we consider this bio-inspired method.

There are three types of molecular communications: diffusion, communication via filaments, and communication via physical contact. Diffusion is a type of molecular communication in which a transmitter releases information molecules to diffuse through the medium freely and reach the receiver. In communication via filaments, a transmitter releases information molecules which will bind to specific molecules known as molecular motors. Molecular motors can attach to filaments and move along them, while carrying information molecules, to reach the receiver. For communicating via physical contact, a transmitter and the receiver should have a physical contact via gap

junctions (a gap junction is an intercellular connection) or synapses. In this type of communication, a transmitter releases information molecules which diffuse through gap junctions or synapses (in the nervous system, a synapse is a structure that permits a neuron (or nerve cell) to pass an electrical or chemical signal to another neuron.) and reach the receiver.

Among the three types of molecular communication, diffusion has attracted more attention ([8, 9, 10]), since communication via filaments and physical contact are not as easy to implement as diffusion. However, there are some drawbacks with the diffusion. Using diffusion process, molecules move in the medium with a low speed, compared to the average speed of motors moving along filaments. Additionally, since there is almost no control over a particle diffusing through a medium, reliability is low and also routing is complex in this scheme of communication. However, a transmitter can control where an information molecule is heading to by picking appropriate filament, or controlling permeability of gap junctions. Further, single receiver communication is not an option in diffusion for the same reason. However, single receiver communication can be carried out in communication via filaments or physical contact. So, although implementation of nano-networks with nodes communicating via filaments or physical contact may not be as easy as using free diffusion, the advantages these techniques have over free diffusion would be worth analyzing. These analyses will lead to more efficient networks in terms of routing, channel capacity, etc. Motivated by these advantages, we started our research work by focusing on nano-networks using molecular communication via filaments and physical contact.

In molecular communication via filaments, it might seem that a transmitter and the receiver should be in direct contact using a filament. However, Moore *et al* suggested using this type of communication in a scenario where a transmitter and a receiver are not in direct contact [11]. This scenario can be considered as wireless communication in traditional communication systems. This new scheme gave molecular communication via filaments an advantage over communication via physical contact, which also had us focus on this type of communication.

The rest of this thesis is organized as follows. In Chapter 2, we investigate three aforementioned molecular communication methods. We first discuss diffusion. Then, we focus on communication via physical contact. This type of communication is divided into two subcategories which will be discussed separately. Finally, we discuss communication via filaments. A system model and a simulation technique are introduced and used to analyze two different

scenarios for this type of molecular communication. In Chapter 3, we introduce nano-relays to enhance performance of nano-networks. A stochastic model based on discrete time Markov chains is proposed to model molecular propagation in this type of communication. Then, the model is modified to capture steady state distribution of information molecules. Chapter 4 presents the results. First, the model is validated by comparing analytic and simulation results. Then, several sets of results are presented to investigate performance of the proposed scenarios. Finally, Chapter 5 concludes the thesis by summarizing our achievements.

Chapter 2

Molecular Communication; Literature Review

Molecular communication is defined as the communication method in which messages are encoded in molecules. This method is a promising candidate for communications in nano-networks. Molecular communication is a method inspired by signaling techniques used in biological systems, specifically human body. Normal functioning of the human body involves a vast diversity of communications occurring simultaneously at the cell level in every organ every millisecond. In spite of the complexity of the human body, intercellular communication (communication among different cells) can be classified into three major groups:

- communication via diffusion (e.g., hormones, growth factors)
- communication via cell contact (e.g., gap junctions)
- communication mediated by the extracellular matrix.

Also, in human body we have intracellular communications (communications that take place inside a cell), which takes place in different ways. One of the most known methods is motoring messages (molecules) on filaments, which is called molecular communication using filaments.

The aforementioned methods are bio-inspired molecular communication methods. Some of them are easier to be used in nano-networks. The first two intercellular communication methods can be easily carried out in a nano-network, but the third one needs a matrix of polymers for the molecules to

attach to and move. Therefore, this method is not the easiest method to be used in nano-networks.

In this chapter, we present a literature review on the first two intercellular, and the intracellular communication methods. We start with diffusion. Then, we explain molecular communication via physical contact, and finally, we investigate molecular communication using filaments. In this thesis, we use molecular communication and nano-communication interchangeably. Table 2.1 summarizes the molecular communication methods discussed in this chapter.

Table 2.1: A summary of discussed molecular communication methods in this chapter.

Communication method	**Information career**	**Short description**
Molecular communication via diffusion	Diffusing molecules	Information molecules diffuse in the channel to move from a transmitter to the receiver.
Molecular communication via gap junctions	Diffusing molecules	Information molecules diffuse through gap junction from a transmitter to the receiver.
Neurospike communication	Diffusing molecules	Information molecules diffuse through the synoptic cleft and reach the receiver which is already stimulated by neurotransmitters.
Molecular communication via filaments	Molecular motors	Molecular motor moves on a filament that connects a transmitter and the receiver, while carrying the information molecule.

Molecular communication in a rectangular channel	Microtubules	An information molecules is loaded to a microtubule which moves towards the receiver on a plane of motors.
Molecular communication in free space	Molecular motors	A hybrid of molecular communication via diffusion and molecular communication via filaments.

2.1 Molecular communication via diffusion

Diffusion is defined as the transport of molecules from a location with higher concentration, to a location with lower concentration. Assume that a transmitter emits Q molecules of type A. Fick's law proposes the well-known formula explaining the concentration of the released molecules at a location in distance r from the transmitter in a three dimensional space as follows [12]

$$C_{r,t} = \frac{Q}{\sqrt{6\pi Dt}} exp(\frac{-r^2}{6\pi Dt}), \tag{2.1}$$

where, D is called diffusion coefficient (which depends on the physical properties of the medium and the emitted molecules).

In molecular communication via diffusion, a transmitter releases molecules which diffuse through the medium. When the molecules reach a receiver, the receiver senses them and decodes the message. The first step to investigate this process is to characterize diffusion in a channel. Llatser *et al.* [13] find characteristics of a communication channel using diffusion. They use (2.1) to calculate the impulse response, pulse width, and pulse delay of a signal if the transmitter releases Q molecules. Putting derivative of (2.1) equal to zero, they find the peak value of the concentration at the receiver location and compute the pulse width for 50% of this value. Having calculated the pulse width, finding pulse delay is straightforward.

Several modulation techniques are proposed for molecular communication via diffusion. Kuran *et al.* [14] propose concentration shift keying (CSK) and molecule shift keying (MoSK) as two modulation techniques. In CSK (see the Appendix for a full list of abbreviations), the concentration of the emitted molecules is used as the amplitude of the signal. The receiver decodes the

intended symbol as 1 if the number of information molecules arriving at the receiver during a time slot exceeds a threshold, and decodes 0 otherwise. MoSK is another technique Kuran *et al.* propose. In this technique, type of the emitted molecules are used to modulate messages. Of course, this technique can be used to send multiple bits at once. For example, four types of molecules can be used to transmit two bits.

In another study, Mahfuz *et al.* [15] investigate performance of CSK by considering an ON-OFF case where molecules are emitted by the transmitter if the transmitted message is 1, and are not emitted if the message is 0. Then, they propose a new modulation technique. They assume that the transmitter emits molecules in a sinusoidal pattern. In this case, the information can be encoded in the changes in the input modulated concentration or in the frequency value of the input. For instance, multilevel amplitude modulation (M-AM) can be obtained if the concentration is modulated by varying the amplitude of the sinusoidal, while frequency shift keying (FSK) modulation can be performed if the carrier is modulated by varying the frequency of the sinusoidal concentration signal.

Inter symbol interference (ISI) is a significant issue in molecular communication. Mahfuz *et al.* [10] analyze their proposed modulation techniques for this issue. The important parameters that affect ISI in this method are communication range and data rate of the system. The effects of these parameters on the ISI is investigated and it is shown that depending on the scenario, channel parameters should be selected carefully to achieve low ISI. Of course, more research works on molecular communication via diffusion can be found in the literature, for example in [9, 16, 17].

2.2 Molecular communication via physical contact

Nano-communication via physical contact can be carried out via gap junctions or synapses. For communication via gap junctions, we define a system model, introduce two channel models, and report some experimental results. Then, we discuss nano-communication using synapses, which is know as neurospike communication by introducing two channel models and a collision-based ad-hoc protocol. Some experimental results for neurospike communication conclude this section.

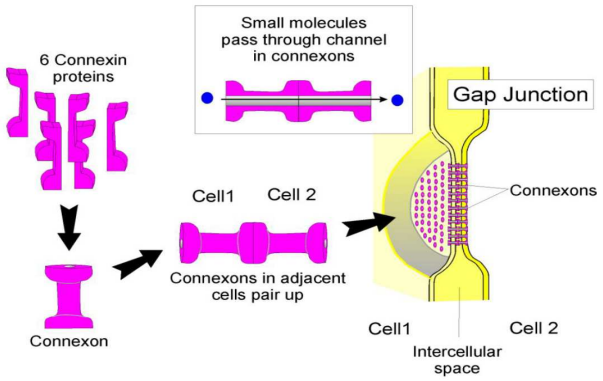

Figure 2.1: Gap junctions structure.

2.2.1 Molecular communication via gap junctions

Gap junctions are considered as cell adhesion junctions and cell-cell communicating junctions. In this section, we focus on the communicating performance. However, based on the structure of gap junctions, which will be introduced later, it will be clear that they can have a role in cell adhesion.

Gap junctions are made up of clusters of closely packed connexons. A connexon is a trans-membrane channel which can dock with a connexon in an adjacent cell. Connexons are hexameric, they consist of arrays of 6 subunits. These sub units are called connexins, which are proteins. Connexins are different types and a connexon may be made of the same or different types of connexins. It is shown, through experiments, that connexins can spontaneously form connexons. Figure 2.1 summarizes the above discussion[1].

Molecules of small size can diffuse through the connexons from one cell to another. However, permeability of the connexons could be regulated to control the molecules which diffuse through the channel. A protein in human body, named MAPK, phosphorylates connexins and makes them incapable of forming permeable channels.

Gap junctions have important roles in heart function. Cardiac muscles are comprised of a multitude of cells that can only communicate via gap junctions. Thus the number, size and localization of these gap junctions are critical to normal heart function.

[1]Figure 2.1 is borrowed from lecture notes of the course " human cell biology , Dr.D Oday, University of Toronto, Mississauga.

System model

Nano-communication via gap junctions, like any other communication process, involves encoding, sending, propagation, receiving, and decoding ([18, 19]). We discuss each as follows:

- **Encoding**: Encoding is the process in which a transmitter translates an external message into a message which could be expressed in the channel; for instance, selecting proper characteristics of a Ca^{2+} (Calcium with two positive charges) wave based on the intended message. Of course, any other type of ions or molecules may be used for encoding in a general nano-network. Inspired by classical AM and FM modulations, different ways of encoding data using Ca^{2+} waves is proposed. More specifically, a message may be encoded in the amplitude or the frequency of a calcium wave [15].

- **Sending**: Sending is the process of generating a wave of molecules. A transmitter can store ions of Ca^{2+} and release them in appropriate patterns. Also, a transmitter might release other molecules which stimulate neighboring cells to release Ca^{2+}.

- **Propagation**: A generated wave can propagate through gap junctions from a nano-machine to another nano-machine. If the number of gap junctions connecting neighboring nano-machines is large enough, propagation could be approximated by free diffusion. Otherwise, we need new models to capture characteristics of diffusion with appropriate boundary conditions.

  Wave propagation may be guided by controlling permeability of gap junctions. Using this property, nano-machines can carry out several functionalities. The most important one is signal switching or routing [19]. Of course, detailed algorithms to perform this type of routing is needed. Signal aggregation is another functionality. If one nano-machine is not capable of generating a specific amount of ions concentration, other nano-machines may help him by controlling their gap junctions to add up generated waves by them [19]. Detailed algorithms for this functionality is also needed. In addition to what was mentioned, repeating a signal for compensating attenuation is another functionality [20]. Considering a flux of Ca^{2+} in nano-machines, they can amplify a signal in case the Ca^{2+} concentration in the channel is less than a

portion of the concentration in the flux. Considering free diffusion for the signal, we can manipulate Fick's law to capture this process [20] as follows:

$$\frac{\partial c(x,t)}{\partial t} = D\frac{\partial^2 c(x,t)}{\partial x^2} + u(c(x,t))r(x), \tag{2.2}$$

where, *c(x,t)* is the concentration of Ca^{2+}, D is the diffusion coefficient, *u(x,t)* is the amplification rate, and *r(x)* is the spatial distribution of the repeaters. *u(x,t)* is:

$$u(x,t) = v([Ca^{2+}]_{flux} - [Ca^{2+}]), \tag{2.3}$$

where, v is the leakage rate (from the flux to the channel), $[Ca^{2+}]_{flux}$ is the Ca^{2+} concentration in the flux and $[Ca^{2+}]$ is the Ca^{2+} concentration in the channel.

- **Receiving**: Receiving is the process of sensing the waves. A receiver can receive a Ca^{2+} wave directly, or receive activities of neighboring nano-machines which were caused by the wave (indirect receiving).

- **Decoding**: Decoding is the process of finding the message from the received signal. As an example, if the received signal is a Ca^{2+} wave, the amplitude or the frequency of the wave is used to decode the message [15]. In this case, different levels of the amplitude or the frequency are decoded to different symbols. In the case of indirect receiving, neighboring nano-machines will carry out some activities and the receiver decodes the message based on that. An example for such activities is releasing a special type of molecule which binds to the receiver's surface and stimulates it. Different types of molecules lead to different stimulations, and consequently are decoded to different symbols.

Channel model

One of the most comprehensive investigations on gap junction communication channels is discussed in [21]. Kilinc *et al.* consider two adjacent nano-machines, which have established gap junctions and work similar to the cells in muscular tissue of a heart. Four different states are considered for the communication channel: HH: channels on both nano-machines are open, HL, and LH: one channel is open and the other one is closed, LL: both channels are closed. Since probability of LL happening is low, this state is

ignored. The dynamics of a channel is given by the probabilities of being in different states. In real scenarios, there are several gap junction channels connecting two communicating nano-machines and states of these channels define the overall conductance of the communication channel for the signal propagation. In [21], the conductance threshold for letting the propagation happen is calculated, and the probability that the conductance of a communication channel is above the threshold is derived.

Having defined the model, Kilinc *et al.* [21] use it to perform an information theoretical analysis on the gap junctions channels. They consider the communication channel as a memoryless Binary Asymmetric Channel (BAC) with On-Off Keying (OOK) modulation. Then, the proposed model is used to derive the probability distribution of the transmitted signal conditioned on a received signal, and find the capacity of the channel.

Kilinc *et al.* [21] present useful results. They investigate effect of the number of gap junctions and radius of the nano-machines on the information rate. The results illustrate that increasing number of gap junctions, and decreasing the radius of the nano-machines will increase the channel capacity. In another set of results, the channel delay is investigated. It is shown that increasing the number of gap junctions established between a transmitter and the receiver form 100 to 300, in the considered scenario, will reduce the delay significantly. However, increasing the number of gap junctions more will not have a major effect on the delay. The reason is that increasing the number of gap junctions over 300 will remove the effect of the gap junctions and connects the adjacent nano-machines. Of course, the number of necessary gap junction to have such results is different for different scenarios.

In another study, Nakano *et al.* [18] propose a model for a network of nano-machines communicating via gap junctions. A network of nano-machines can be arranged in a vector or matrix structure. Using vector structure, each nano-machine will communicate with its two neighbors. However, using matrix structure each nano-machine can establish a communication channel with all or some of neighboring nano-machines by controlling permeability of gap junctions. Considering a vector of nano-machines, it is shown in [18] that if the permeability of gap junctions is higher than a threshold, since the topology is linear the wave will propagate to the last end nano-machine without attenuation. Otherwise, the wave will attenuate and nano-machines far from the transmitter cannot sense it.

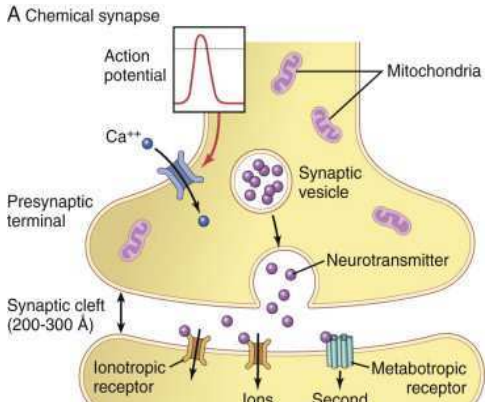

Figure 2.2: Cell signaling using synapses [2].

Reported experimental results

Nakano *et al.* [22] report experimental results for fabricating a microplatform by utilizing photolothography (a process used in microfabrication to pattern parts of a thin film or the bulk of a substrate) and surface chemical treatment. They use already existing biological cells as nano-machines and culture them on the microplatform. Results in [22] show that the implemented gap junctions can guide Ca^{2+} waves.

2.2.2 Neurospike communication

Nervous system uses synapses as one method of communication among cells. In the nervous system, a synapse is a structure that allows a cell to pass a signal to another cell. In this method of cell signaling, a transmitter (presynaptic cell or axon) and the receiver (postsynaptic cell) are 20 to 40 nm apart. The transmitter releases a chemical called neurotransmitter that diffuses through the gap between transmitter and receiver (synaptic cleft), binds to the receptors located on the membrane of the receiver cell, and stimulates the receiver. Stimulation of the receiver causes it to initiate a pathway that lets message molecules to enter the receiver (Figure 2.2). Figure 2.2 illustrates this cell signaling using synapses structure.

A propagation model for neurospike communication is proposed in [23]. Figure 2.3 shows the block diagram of this model. Gallluccio *et al.* [23] borrowed equations from chemistry and biology to model the channel. In

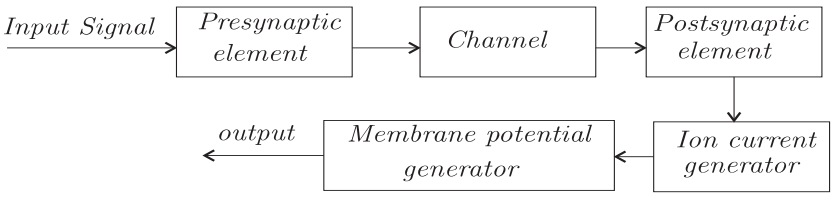

Figure 2.3: Detailed block diagram of communication via synapses.

Figure 2.3, presynaptic block models transmitter stimulation by an external message, translating the message into properties of information molecules or ions (encoding), and releasing the ions and neurotransmitters to the channel (sending). Released ions and neurotransmitters diffuse through the cleft between the transmitter and the receiver (propagation) to the receiver. The channel block in Figure 2.3 models this propagation. Neurotransmitters which have diffused through the cleft and reached the receiver then bind to the receiver's receptors (modeled by postsynaptic block), which in turn results in opening of the valves on the receiver and letting the ions flow into the receiver (receiving process). This process is modeled by ion current generator. The ion flow to the receiver causes changes in the receiver (such as changes in the level of a specific ion) which are captured by membrane potential generator (decoding). This is a comprehensive model that can be used in advanced analyses of nano-networks using neurospike communication. Gallluccio *et al.* then use the same approach and extended the model to a multi-input channel in [24].

Balevi [25] proposes a channel model based on physiological properties of neurons, from a communication point of view. In [25], neurospike communication is divided into two main blocks: axonal communication, and synaptic communication. Axonal communication is considered as the communication process in the axon, and synaptic communication is considered as the communication process through the synaptic cleft. Each block is discussed separately. Having established the blocks, Baleyi proposes a physical channel model and finds input-output relation of the channel for the receiving probability of an impulse train. Then, in order to investigate the effect of interference, he extends the model to a multi-input, single output model. Since a transmitter with low transmission rate has a high error probability in such a channel (other transmitters has high rates and release information molecules with high rate which cause interference with high probability), Baleyi defines a technique such that synaptic weights of the inputs are adjusted so that the

input with lower rate is not lost among strong inputs. The synaptic weight of an input is the effect its neurotransmitters has on the receiver. It could be considered as the channel gain.

A collision based ad-hoc nano-network

In this section, we analyze a collision-based ad-hoc nano-network and derive the information capacity, delay, and throughput of the network. In the considered scenario, nano-machines floating in a volume might collide and adhere, while moving, to establish a communication channel. This process of collision, adhesion, and communication between nano-machines goes on until a generated message reaches a specific nano-machine (infostation).

In [26], collision rate of nano-machines, R_c, is calculated as:

$$R_c \approx \frac{4\pi r^2 E[v_{nn}]}{V}, \tag{2.4}$$

where, r is the nano-machines' radius, $E[v_{nn}]$ is the average relative speed of colliding nano-machines, and V is the volume in which nano-machines are floating.

Colliding nano-machines should then adhere to establish a channel. Adhesion is assumed to happen via binding of molecules on the surfaces of the two nano-machines. Considering $p(t)$ as the probability of forming one bond at time t (which could be derived based on chemical equations [26]), probability of forming n bonds is:

$$p_n(t) = \binom{A_c m_{min}}{n} [p(t)]^n [1 - p(t)]^{A_c m_{min} - n}, \tag{2.5}$$

where, A_c is the area of contact of nano-machines and m_{min} is the minimum surface density of bonding molecules. So, if adhesion of nano-machines needs minimum of c bonds, the probability of adhesion at time t, $p_a(t)$, is:

$$p_a(t) = 1 - \sum_{i=0}^{c-1} p_i(t). \tag{2.6}$$

Adhered nano-machines will then communicate via synapses. Guney *et al.* [26] introduce a model for the synapses channel. Figure 2.4 shows the block diagram of this model. The transmitter releases neurotransmitters to

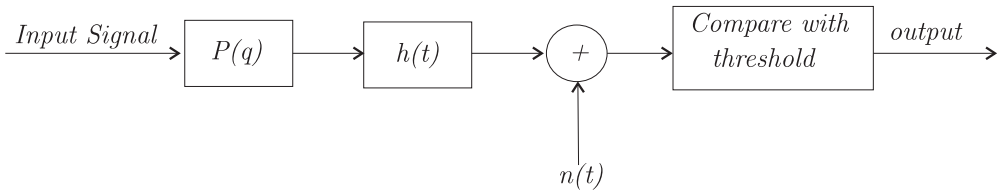

Figure 2.4: Block diagram for neurospike communication.

diffuse through the cleft between the transmitter and the receiver, bind to the receiver, and cause the valves on the receiver to open. This will let the information molecules flow, generated by the transmitter, into the receiver. The shape and amplitude of the flow is captured in *h(t)* and q, respectively ($P(q)$ is the probability distribution of q). This process may be noisy because of presence of other types of molecules or even thermal noise.

First, let us derive the mutual information. A transmitter releases neurotransmitters and ions as bit 1, and does not as bit 0. The receiver then decides on the received signal. The receiver compares the correlation of fluctuations in the voltage of its membrane caused by the ions flow (response to the ions flow) and a predefined signal (*h(t)*), with a threshold to decide on the received bit [26]. Considering r as the correlation, Y as the received signal, and θ as the threshold:

$$\begin{aligned} r \geq \theta \Rightarrow Y = 1, \\ r \leq \theta \Rightarrow Y = 0. \end{aligned} \tag{2.7}$$

This decision is not always correct. Transmitted bit may be 1 but the receiver decodes 0 (miss detection), or vice verse (false alarm). Miss detection (P_M) and false alarm (P_F) probabilities are as follows [26]:

$$P_F = \frac{1}{2}(1 - erf(\theta)), \tag{2.8}$$

$$P_M = \frac{1}{2}[1 + \int_0^\infty erf(\theta - q\sqrt{SNR})P(q)dq], \tag{2.9}$$

where, *P(q)* is the distribution of the amplitude of a received signal. Therefore, error probability of a decoded signal will be:

$$P_E = p_1 P_M + (1 - p_1)P_F, \tag{2.10}$$

where, p_1 is the probability of transmitting bit 1.

Based on the above formulation, transition matrix for the channel is:

$$P(Y|X) = \begin{bmatrix} p_1(1-P_M) & (1-p_1)P_F \\ p_1 P_M & (1-p_1)(1-P_F) \end{bmatrix}. \tag{2.11}$$

Therefore, the mutual information is:

$$\begin{aligned} I(X;Y) &= H(Y) - H(Y|X) \\ &= H(p_1 P_M + (1-p_1)(1-P_F)) \\ &\quad -(p_1 H(P_M) + (1-p_1)H(P_F)), \end{aligned} \tag{2.12}$$

where, X is the transmitted signal. Using (2.12) and assuming minimum inter symbol duration of $3ms$, Guney *et al.* [26] calculated maximum capacity of the channel with common parameter values and have derived bandwidth of 190 bps.

Two adhered nano-machines use the established channel and intercommunicate their summary vectors (which indicates if the nano-machine is carrying the message). If one of the nano-machines is not carrying the message, the one with the message will transmit it to the other. This strategy is similar to the epidemic routing scheme for partially-connected ad-hoc networks [27]. This goes on until the message reaches the infostation. The average time from generating a message in a nano-machine to reaching the infostation is defined as the average delay time (T_d).

In [26], an absorbing Markov chain is introduced to derive the average delay time of the system. Figure 2.5 shows the Markov chain. *S(t)*, *I(t)*, and *R(t)* define the number of nano-machines without the message, the number of nano-machines carrying the message, and the number of nano-machines which passed the message to the infostation (either 0 or 1), respectively. The process starts at state S and gets absorbed to state R. Assuming total number of N nano-machines, each nano-machine may collide, adhere and communicate with $\beta(N-1)$ other nano-machines in a time unit, where β is the rate of spreading information among nano-machines. Consequently, β is defined as:

$$\beta = R_c \times p_a \times R_t, \tag{2.13}$$

where R_t is the probability that an n bit message is successfully received:

$$R_t = (1-P_E)^n. \tag{2.14}$$

Probability that a nano-machine carrying the message collides, and communicates, with another nano-machine not carrying the message, conditioned

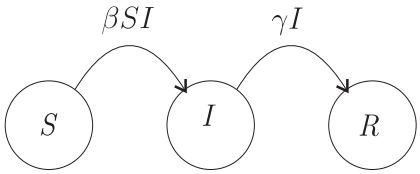

Figure 2.5: Markov chain model for message spreading.

on that a collision has happened, is $\frac{S_N}{N-1}$ (where S_N is the number of nano-machines in the state S). Also, all the nano-machines carrying the message may collide with any of the nano-machines not carrying the message. Therefore, transit rate from the state S to the state I in the Markov chain will be $\beta(N-1)\frac{S_N}{N-1}I_N = \beta S_N I_N$ ((where I_N is the number of nano-machines in the state I)).

Similarly, let us define γ as the rate at which a nano-machine collides, adheres, and transmits a message to the infostation. So, transition rate from the state I to the state R in the Markov chain is γI_N. γ is calculated as:

$$\gamma = R_{ic} \times p_a \times R_t, \tag{2.15}$$

where, R_{ic} is the rate of collision with the infostation. Considering (2.4), R_{ic} is:

$$R_{ic} \approx \frac{\pi(r + r_i)^2 E[v_{ni}]}{V}, \tag{2.16}$$

where, r_i is the radius of the infostation and $E[v_{ni}]$ is the average relative speed of nano-machines and the infostation [26].

If $F(t) = Pr(T_d < t)$, then:

$$\begin{aligned} &Pr(T_d > t + \epsilon | T_d > t) \\ &= 1 - Pr(t < T_d < t + \epsilon | T_d > t) \\ &= 1 - \epsilon\gamma I_N(t). \end{aligned} \tag{2.17}$$

So:

$$\begin{aligned} &Pr(T_d > t + \epsilon) \\ &= Pr(T_d > t) Pr(T_d > t + \epsilon | T_d > t) \\ &= Pr(T_d > t)(1 - \epsilon\gamma I_N(t)). \end{aligned} \tag{2.18}$$

Using (2.18), a differential equation for $F(t)$ can be derived as follows:

$$\begin{aligned}\frac{dF}{dt} &= \lim_{\epsilon \to 0} \frac{[1 - Pr(T_d > t + \epsilon)] - [1 - Pr(T_d > t)]}{\epsilon} \\ &= \gamma I_N(t) Pr(T_d > t) \\ &= \gamma I_N(t)[1 - F(t)]. \end{aligned} \tag{2.19}$$

To solve the differential equation (2.19), $I_N(t)$ is needed. It is calculated using the transient solution of the Markov chain, as:

$$\begin{aligned}&\frac{dI_N(t)}{dt} = \beta S_N I_N = \beta N I_N - \beta {I_N}^2 \\ &\Rightarrow I_N(t) = \frac{N}{1 + (N-1)e^{-\beta N t}}. \end{aligned} \tag{2.20}$$

Noting that $F(0)$ (initial condition) defines the probability that the nano-machine initiating a message propagation is already adhered to the infostation, $F(0)$ will be defined as follows:

$$F(0) = \frac{\frac{4}{3}\pi(r_i^3 - r^3)}{V}. \tag{2.21}$$

Solving the differential equation (2.19), with initial condition (2.21), *F(t)* can be calculated. Calculating $F(t)$, T_d will be:

$$T_d = \int_0^\infty 1 - F(t) dt. \tag{2.22}$$

Closed form solution of (2.22) for a special case is derived in [26].

As for the throughput of the system, since it takes T_d units of time to deliver a message of n bits to the infostation, the average throughput of the network is calculated as:

$$Th_{avg} = \frac{n}{T_d}. \tag{2.23}$$

Using the model discussed above, some interesting results are derived in [26]. It is shown that increasing the speed and size of nano-machines and infostation will decrease the average message delivery delay and increase the average throughput. Also, it is shown that increasing θ, will decrease the average delay and increase the average throughput to a point, and then it will have a reverse effect. It is because increasing θ reduces false alarm probability and increases miss detection probability. Therefore, there is an optimum θ. It is worth mentioning that the optimum θ depends on SNR.

Reported experimental results

Balasubramaniam *et al.* [28] have developed experiments to design an interface which is capable of communicating with neurons. The results show that the interface they used activates signaling process in neurons.

2.3 Molecular communication via filaments

Filaments are rope-like polymers,[2] which can grow as long as 25 micrometers and are highly dynamic. The outer diameter of a filament is about 20 nm. Filaments are important for maintaining cell structure, providing platforms for intracellular transport, as well as other cellular processes. There are many proteins that bind to filaments, including motor proteins such as kinesins and myosins, and use theme as an infrastructure to move.

Filaments make an infrastructure for molecular motors to move molecules inside cells. Molecular motors can bond to the cargo and move along filaments. They have two heads which bind to filaments using ATP[3](Figure 2.6). In order to walk, one of ATP molecules hydrolysis[4] and changes to ADP,[5] which can not bind to filaments. Therefore, the motor has one free head which can move. The free head moves forward; meanwhile ADP is replaced by an ATP that present in the cell. Now, the free head had one step forward and has an ATP which can be used to bind to the filament again (Figure 2.6). This process keeps going and the motor moves along the filament[6]. In this research work, we assume there are enough ATPs in the medium for molecular motors to move.

Filaments have two distinct ends, which are presented as +ve and -ve. If a molecular motor attaches to a filament it may move towards the +ve end or the -ve end, depending on the type of the motor (structure of the motor defines the direction). For example, myosin 6 move towards -ve end of a filament and most other myosins move toward the +ve end [29]. Therefore, we can have a two way path for moving cargoes by switching between these two type of molecular motors .

[2] A polymer is a large molecule composed of repeating structural units

[3] ATP is a molecule used in cells for different purposes

[4] Hydrolysis means the rupture of chemical bonds by the addition of water

[5] Another useful molecule in cells

[6] Although this model is widely accepted, there are differing views in literature on how molecular motors move along filaments.

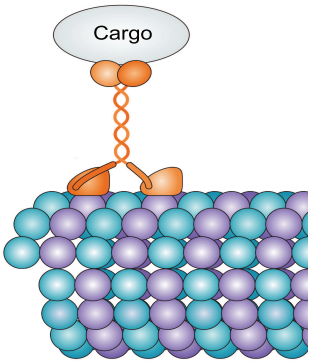

Figure 2.6: Molecular motors moving along filaments [3].

Having defined filaments and molecular motor, we present a literature review on molecular communication using filaments. We first introduce a system model for this type of communication. Then, as simulation approaches are common in analyzing a system, we discuss how simulating communication via filaments is carried out. Afterwards, we introduce two common scenarios considered in the literature and discuss different network parameters for each scenario. Some experimental results form the last part of the literature review for molecular communication using filaments.

System model

Nano-communication via filaments needs several components: transmitter, receiver, filaments, information molecules, and molecular motors to carry information molecules along filaments [30]. Using these components, communication process involves encoding, sending, propagation, receiving, and decoding [31]. We discuss each briefly:

- **Encoding**: Encoding is the process in which a transmitter converts a message into some characteristics of information molecules. For example, the number of released molecules could be used to encode a message. In this example, a transmitter can transmit a two bit message with maximum of three released molecules at a time (sending no molecule is also one state).

- **Sending**: Sending is the process of releasing information molecules into

a channel. A transmitter can release information molecules already attached to molecular motors, or information molecules which then attach to molecular motors in the channel.

- **Propagation**: Propagation is the process of transmitting information molecules from a transmitter to the receiver. Molecular motors carry out propagation by carrying information molecules while moving along filaments. It is worth mentioning that in case a molecular motor is not attached to a filament, it will diffuse through the medium and wherever it finds a filament, it will attach to the filament and start moving along it.

- **Receiving**: Process of retrieving information molecules attached to the molecular motors.

- **Decoding**: Receiver can decode the message using the information molecules. Considering the example mentioned for encoding, receiver can decode the message by counting the number of received information molecules.

2.3.1 Simulating molecular communication via filaments

It is straightforward to simulate particles diffusing through a medium, since diffusion has a closed form mathematical formulation. However, moving along filaments does not have such a formulation and is not as straightforward as simulating diffusion. In this section, we present an approach to simulate molecular movement along filaments in a specific scenario. One can develop the technique for other scenarios.

We describe the simulation technique presented in [32]. In this technique, Farsad *et al.* consider an inverted geometry in which filaments move over stationary molecular motors in a two dimensional plane (they assume information molecules can use DNA strings to attach to filaments). The plane is fully covered by molecular motors so that filaments would be able to move in different directions. Considering the x and y coordinates and Δx_i and Δy_i for movement on along the coordinates, the displacement of the ith step in the x direction and the y direction, as:

$$\Delta x_i = \Delta r_i \cos\theta_i, \tag{2.24}$$

$$\Delta y_i = \Delta r_i \sin\theta_i, \tag{2.25}$$

where Δr_i is the displacement, and θ_i defines the direction. Δr_is are independent identically distributed (iid) Gaussian random variables with mean and variance of:

$$E[\Delta r] = v_{avg}\Delta t, \tag{2.26}$$
$$Var[\Delta r] = 2D\Delta t, \tag{2.27}$$

where v_{avg} is the average speed of a filament, D is the diffusion coefficient of the medium, and Δt is the time step. θs are correlated in the manner as:

$$\theta_i = \theta_{i-1} + \Delta\theta, \tag{2.28}$$

where $\Delta\theta$ is an iid Gaussian random variable with mean and variance of:

$$E[\Delta\theta] = 0, \tag{2.29}$$
$$Var[\Delta\theta] = \frac{v_{avg}\Delta t}{L_p}, \tag{2.30}$$

where L_p is the persistence length (a through study on persistence length can be found in [33]). Sample values for v_{avg} and L_p are $0.85\mu m/s$ and $111\mu m$, respectively. Since the distributions of Δr_i and $\Delta\theta$ are known, they can be used to find Δx_i and Δy_i, and consequently, the new position of the particle for the next step.

In a bounded channel, a filament may collide with the boundaries while moving. In this case, the filament can either follow the boundary or reflect off it. In the case of following the boundary, the next step would be taken along the boundary and for steps after that, direction is randomly chosen from possible options. In the case the filament reflects off the boundary, if θ_h is the hitting angle, the next step direction angle is $2\theta_h$ and then direction is randomly chosen from possible options.

Loading information molecules to filaments should be carried out at the transmitter position, and unloading should be carried out at the receiver position. As mentioned earlier, transmitter can release just information molecules or molecules already attached to filaments (since in this section it is assumed filaments are moving along molecular motors). In case information molecules are already attached to filaments, they can start propagation immediately. Otherwise, Farsad *et al.* [32] suggested a loading process (sending process). They considered a loading zone around the transmitter. Released information molecules will be anchored to the loading zone until being loaded to a

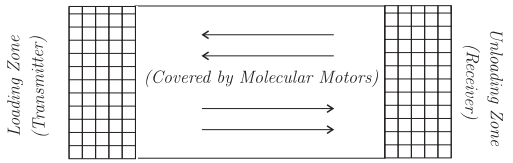

Figure 2.7: Considered bounded channel. The hatched parts represent the loading and unloading zones. Filaments movie towards the loading an unloading zones, as shown by the arrows.

filament. To simulate this process, one can divide loading zone to a square grid and put each information molecule in one of the grids randomly. If a filament gets close to a grid during its movement, it can load the information molecule. Likewise, an unloading zone is considered. When a loaded filament gets to the zone, it will unload the information molecule and the receiver can sense that.

2.3.2 Molecular communication in a rectangular channel

In this section, we consider a scenario with an inverted geometry where a two dimensional bounded rectangular channel is covered with molecular motors. The transmitter and the receiver are at the two ends of the channel. Filaments move in the channel on the motors and transport information molecules from the loading zone to the unloading zone. We call the scenario nano-communication in a rectangular channel. Figure 2.7 illustrates the topology. Simulation method discussed in Section 2.3.1 can be applied to this scenario.

In this scenario, the message intended to be transmitted is encoded in the number of released information molecules. For example, a two bit message can be encoded by releasing 0,1,2, or 3 molecules to the loading zone at a time. The filaments carry released molecules to the unloading zone in T seconds (intersymbol duration). Then, the receiver counts the number of the received molecules, decodes the message, and removes the molecules from the channel. We should mention that in the considered scenario, filaments hitting the boundaries will follow the boundary.

Eckford *et al* [34] find if the proposed communication method surpasses free diffusion, as a reference, in terms of mutual information. If x is the

number of released molecules to the loading zone and y is the number of molecules in the unloading zone after T seconds, mutual information is:

$$I(X,Y) = E_{x,y}\left[log_2 \frac{p(y|x)}{\sum_x p(y|x)p(x)}\right], \tag{2.31}$$

where p defines probability mass function. $p(y|x)$ is defined for both techniques.

Probability of first passage time in T seconds for a particle diffusing in a medium has been derived in [35]; let us call it p_a. So, p_a is the probability that a molecule diffuses through the channel and reaches the receiver zone in T seconds. Therefore, probability of y molecules out of x reaching the receiver is:

$$p(y|x) = \binom{x}{y}(p_a)^y(1-p_a)^{x-y}. \tag{2.32}$$

For communication using filaments, $p(y|x)$ can be defined by running simulations for several times. It is worth mentioning that it is assumed molecules will be removed from the channel after each T seconds. This is the ideal case where intersymbol interference is canceled. We will elaborate on molecule removal processes proposed in the literature in Section 2.3.3.

It is clear that the number of times a filament can move between the loading and the unloading zone in T seconds is limited. Since the path a filament follows is not fixed, this number is a random variable. But it has a maximum value (if the filament goes through paths in parallel with the channel border.) Results in [34], which we have also reproduced (generating similar results was a good way to understand the details and issues of different molecular communication methods. We used MatLab to reproduce the results.), show that the maximum is an important factor defining information rate of the system. Assuming just one filament in the channel, if the number of released molecules exceeds this maximum, since the filament carries one information molecule at a time, it cannot carry all the released molecules to the unloading zone before the next symbol, and this will cause error in the decoded message. Based on the results in [34], using filaments will give a higher capacity than free diffusion if the number of released molecules is less than the maximum number of times a filament can move between loading and unloading zones in T seconds. Otherwise, using diffusion based communication is beneficial.

In [34], no drift is considered for the diffusion process. Farsad *et al.* [36] compare molecular communication using filaments and diffusion with drift.

Considered drift for the molecules in diffusion process is $v = 0.3\mu m/s$ towards the unloading zone (channel dimensions are $20 \times 60 \times 10\mu m$). Simulation results show that for the considered scenario and in terms of information rate, using diffusion process with drift outperforms both diffusion without drift and using filaments. We should note that this result means there is a scenario under which diffusion with drift is the best choice for maximizing information rate, but it is not general. Changing the drift, for example, would affect the results.

Farsad *et al.* [34] calculated information rate of the system using simulation results. Moving from simulation to analytic models, an estimation for conditional probability distribution of the received signal will be derived, based on which one can calculate information rate of a channel [37]. This model is not totally analytic and needs some simulation results. However, since simulating the whole behavior of a channel is not needed in the model, it helps in calculating information rate of a channel fast. Consider N as the number of grids in a gridded loading zone, X as the number of released molecules to the loading zone, and X_i as a random variable equal to 1 if the *ith* grid in the loading zone is occupied by a molecule, and 0 otherwise. Assuming X_is are independent and identical:

$$p\left(X_i = 1\right) = \frac{X}{N}. \tag{2.33}$$

Also, let V_i be another random variable equal to 1 if a filament visits the *ith* grid in the loading zone during its transition from the unloading zone to the loading zone, and 0 otherwise. $p\left(V_i = 1\right)$ and $p\left(V_i = 0\right)$ can be derived by simulation. Define V_i^k as a random variable equal to 1 if the *ith* grid is visited at least once during k transitions of a filament, and 0 otherwise. Then:

$$p\left(V_i^k = 1\right) = 1 - \left(1 - p\left(V_i = 1\right)\right)^k. \tag{2.34}$$

Let D_i^k represent the event that a molecule in the *ith* grid is transmitted to the unloading zone in k transitions of a filament. Assuming X_is and V_is are independent:

$$p\left(D_i^k = 1\right) = p\left(V_i^k = 1\right) p\left(X_i = 1\right). \tag{2.35}$$

Having derived the distribution of V_i and X_i, one can find probability distribution of D_i^k. Now, if Y^k represents the total number of received molecules in k transitions of a filament:

$$Y^k = min\left(\sum_{i=1}^{n} D_i^k, X\right), \tag{2.36}$$

for a given X. So, using Eq.(2.36) one can calculate $p(y|x)$ as:

$$p(y|x) = \sum_{k} p\left(Y^k|X\right) p(k), \tag{2.37}$$

where *p(k)* is the probability that a filament goes through k transitions in an intersymbol time (and can be derived by simulation). Using Eq.(2.37) and Eq.(2.31), one can calculate mutual information and capacity of the channel. In [37], it is shown that this model will provide more accurate results by reducing time per channel use.

Having calculated information rate, Farsad *et al.* [32] propose an optimized channel to maximize it. In order to do so, they consider channel dimensions which have significant effects on the information rate. It is shown in [32] that fixing area of the channel, the shorter the length of the channel, the more the number of filament's transits between the loading and the unloading zones would be, which results in higher information rate. On the other hand, it is shown in [37] that molecules anchored close to the boundaries of the loading zone are met by filaments with higher probability than other molecules anchored somewhere else. Therefore, fixing the area and decreasing the width of the channel will increase the probability of loading a molecule. Based on the simulation results in [32], which we have also reproduced, the scenario with the best performance is the one which makes a trade off: square channel.

The simulation results for the optimized channel are confirmed by an analytic model proposed in [38]. Farsad *et al.* [38] use an analytic method to optimize channel dimensions. Assume length, width, and height of a rectangular channel are l,w, and h, respectively. Considering C as the concentration of filaments in the channel, if S represents the number of transitions between the loading and the unloading zones a filament goes through in T seconds, it is shown in [38] that:

$$E\left[S\right] \approx \lfloor \frac{v_{avg}T}{P} \rfloor, \tag{2.38}$$

where P is the perimeter of the channel. So, the average number of transitions of all filaments will be:

$$E\left[K\right] = VC\lfloor \frac{v_{avg}T}{P} \rfloor, \tag{2.39}$$

where V is the volume of the channel ($l \times w \times h$).

As mentioned earlier, fixing T and maximizing the number of filaments' transitions between the zones will maximize the information rate. So, the

optimization problem will be:

$$max\left(E\left[K\right]\right), \tag{2.40}$$

$$= max\left(VC\lfloor\frac{v_{avg}T}{P}\rfloor\right). \tag{2.41}$$

Fixing h, the optimization problem is maximizing a multiplication over a summation ($\frac{V}{P}$). So, $w = l$ is a constraint for the optimization problem (we had this result before). Using this criterion, Eq.(2.39), and the fact that flooring in Eq.(2.39) bounds increase of the perimeter, one can find the optimum l and w. In [38], this analytic model is validated by simulation results and it is shown that when time per channel use is of order of a few minutes, it gives satisfactory results. Also, in a more advanced study, Farsad *et al* [39] use a similar technique to find the optimized shape for the channel, among rectangular channel, polygon channel, and polygon ring channel. They find that rectangular channel is the optimal channel shape among these three.

Until now, we assumed information molecules attach to filaments without any kind of shield. Farsad *et al.* [40] suggested to put information molecules in vesicles (a structure like cell membrane, made of lipids). This will help in two ways. First, information molecules in vesicles are protected from possible reactions with environment which may change them. Second, since the size of vesicles can be large, the probability that a filament visits a vesicle at the loading zone is high.

Assume information molecules are in an aqueous medium. Vesicles load a volume of the liquid and attach to filaments to be carried to the unloading zone. Fixing concentration of information molecules, optimal vesicle size is derived in [40]. It is shown that for the considered scenario, the larger the size of vesicles, the more average number of information molecules would be transmitted. On the other hand, larger vesicles will lead to the higher variance for the number of transmitted information molecules, which will cause high error probability. Therefore, there is an optimum vesicle size for a system.

2.3.3 Molecular communication in free space

In this section, we are going to introduce a realistic scenario for molecular communication using filaments. In the scenario, a transmitter and the

receiver are between two parallel surfaces apart from each other. The communication technique used in this scenario is a hybrid of free diffusion and moving along filaments. Information molecules released from the transmitter are already loaded to molecular motors (we may refer to information molecule-molecular motor pair as released molecule). If a released molecule is not attached to a filament, it freely diffuses through the channel and in case it reaches a filament, it will attach to the filament. Also, a molecular motor moving along a filament may randomly detach from the filament in each step. We call the scenario nano-communication in free space. During the analyses presented in this section, we will consider different topologies for the filaments.

First, let us find the probabilities that released molecules reach receivers placed in different distances from the transmitter [41]. This type of communication is efficient if these probabilities are high enough. Assume four 20 μm long filaments are attached to the receiver. Simulations in [41] show that if a transmitter and the receiver are 1 μm apart, a released molecule will reach the receiver with satisfactory probability of 0.8. Increasing the distance between a transmitter and the receiver will reduce the probability of a released molecule reaching the receiver. Also in [41], communication using filaments in the considered scenario is compared with diffusion as a reference. Simulation results in [41], which we have also reproduced, show that in terms of the arrival probability of a released molecule to the receiver, it outperforms diffusion based communication significantly.

Next, let us consider an extended version of the scenario mentioned above where polarity of the filaments is taken into account [11]. In this scenario, filaments are considered in different topologies: randomly distributed (noted by M), making asters of size four (asters are structures shaped like stars) where center of the aster is the + end of the filaments (M+), and making asters of size four where center of the aster is the - end of the filaments (M-). Figure 2.8 illustrates the topologies. Moore *et al* [11] use molecular motors which move toward + end of a filament. In order to reduce probability of detaching a motor from a filament, the authors assume each information molecule is attached to several motors which might attach to several filaments independently. Also, assume the transmitter is at the middle of the two parallel surfaces. As for the receivers, they are considered in different topologies: randomly distributed (R), on the + end of each filament (R+), and on the - end of each filament (R-). The number of filaments and receivers in different topologies are the same.

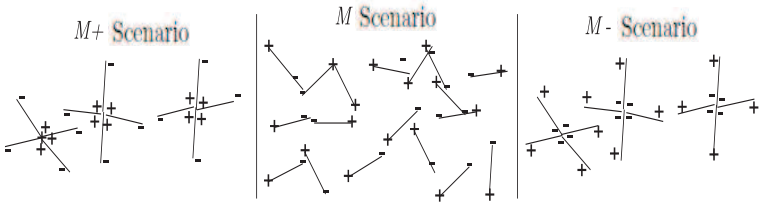

Figure 2.8: Different topologies for filaments. If a molecule reaches a filament (black lines), it starts to move along it, toward the + end. Assuming the receiver is set at the + end, it will receive the molecule.

Simulations in [11], which we have also reproduced, show that using R+ scenario will increase the probability of an information molecule reaching the receiver. Also, using R+ topology, performance of M, M+, or M- scenarios are the same. Considering that motors used in these simulations walk toward + end of filaments, this is what was expected.

The number of filaments in a channel might affect the performance of the system. Based on the results in [42], which we have also reproduced, increasing the number of filaments in the aster can increase probability of receiving an information molecule in an (R+, M+) topology, if the transmitter and the receiver are close. As the distance between them increases, diffusion (before attaching to a filament) becomes the dominant part of the propagation. Therefore, increasing the number of filaments does not have much effect.

In [43], the information rate of an (R+, M+) scenario is compared with two other scenarios where a transmitter and the receiver are connected via filaments, and information molecules diffuse in the channel to reach the receiver. In all the scenarios, a transmitter releases one information molecule already attached to a motor as bit 1, and does not as bit 0. Intersymbol duration is T.

In order to find the information rate, we need mutual information formula, which is defined in (2.31). Writing $p(x)$ and $p(y|x)$ for different values of x and y, we have:

$$p\left(x=0\right)=p\left(x=1\right)=0.5, \tag{2.42}$$
$$p\left(y=1|x=0\right)=n, \tag{2.43}$$
$$p\left(y=0|x=0\right)=1-n, \tag{2.44}$$
$$p\left(y=1|x=1\right)=s+n-sn, \tag{2.45}$$
$$p\left(y=0|x=1\right)=1-\left(s+n-sn\right), \tag{2.46}$$

where s is the probability that a released information molecule reaches the receiver in T seconds, and n is the probability that the receiver receives it after T seconds. These two probabilities can be found by simulation. Having these probabilities in hand, it is straightforward to find the information rate. It is shown in [43] that among three scenarios mentioned, connected transmitter and receiver has the highest information rate. Hybrid scenario (R+, M+) is next, and diffusion can be used where the distance between a transmitter and the receiver is short.

Noise affects information rate in communications. To elaborate on the effect of noise in molecular communication, let us consider a channel in which information molecules are not removed from it after the symbol durations are finished (a channel with no noise removal mechanism). The molecules left in the channel diffuse through it, and might reach a receiver. Because in most known scenarios molecules released by a transmitter are of the same type (the message is coded in the number of released molecules and not the type of molecules), the receiver cannot distinguish whether a received set of information molecules refers to the current message or not. So, it considers the molecule as a released molecule representing the current message, which will cause error in the decoding. Therefore, molecules referring to previous messages which are left in the channel are considered as noise.

Moore *et al.* [43] discuss the effect of noise in molecular communication. According to them, among three scenarios mentioned above (hybrid scenario (R+, M+), a transmitter and the receiver are connected via filaments, and communication using free diffusion), hybrid scenario is the most vulnerable one to the noise. The gap between ideal scenario where information molecules are removed from the channel after T seconds (no matter has reached the receiver or not) and the scenario with no noise removal mechanism where molecules are left in the channel, is large.

Noise reduction is the process of removing molecules not representing the current message from the channel. Moore *et al.* [42] suggest two techniques for noise reduction: exponential decay (noted by E) and receiver removal (R). Using E, information molecules will decompose in the channel after a specific period, and using R, receivers remove information molecules. Simulation results in [42] show that noise does not have any significant effect on the information rate if a transmitter and the receiver are connected (as was shown in [43]). That is because a received molecule detaches from the filament, and diffuses away from the receiver with high probability. But noise has major effect in a hybrid scenario. Results in [42] show that using the noise removal

techniques increases the information rate in a hybrid scenario. Based on the results, performance enhancement for the two noise removal techniques is the same.

Reported experimental results

Hiyama *et al.* [44] present an implemented system using the scenario introduced in Section 2.3.2. They used single stranded DNA-labeled cargoes. Cargoes whose DNA strands are complimentary to those on a filament are loaded to the filament. Reaching the unloading zone, the cargo will be unloaded by binding to a complimentary strand at the unloading zone. Hiyama *et al.* [45] present a similar but more advanced system. They use filaments to move vesicles containing cargoes.

Suda *et al.* [46] implement a nano-network in which - ends of the filaments are glided to transmitters. The + end will randomly grow until it reaches another nano-machine (receiver). They also show that if two filaments overlap with consistent polarity, a molecular motor can switch walking on one filament to another.

Results in [47] may be the most general case. The authors grow filaments on a rail and then put them on a surface to build intended topology of the network. Using this method, one can use a predefined structure for a nano-network in which nano-machines communicate using filaments.

Chapter 3

Propagation Model for Molecular Communication Using Filaments

In this chapter, we first introduce Brownian motion as the mathematical model which describes probability distribution of particles suspended in a liquid. Then, we address an approximation method to find probability distribution of diffusing particles and extend it to approximate Brownian motion with jumps, known as jump diffusion process. We propose using nano-relays to improve the performance of a network in terms of the delay, and use the discussed approximation method to model molecular propagation in molecular communications via filaments. Concluding part of this chapter will be results validating the model.

3.1 Brownian motion

The mathematical model for physical phenomenon of the movement of small particles (of the size of molecules of the medium) is known as Brownian motion. Brownian motion is basically a continuous time continuous space Markov process. In the following, we will investigate this process in detail.

We start this section with an approximation for the movement of a particle. We divide the time axis and the space axis into very large number of intervals. Let us consider τ as time intervals and Δ as displacement step sizes. If a particle starts diffusing from the origin, in each time step it will

take a step, Z, where:

$$prob\{Z = +\Delta\} = p, \quad prob\{Z = -\Delta\} = q. \tag{3.1}$$

Therefore, moment generating function of each step can be derived as:

$$E\left\{e^{-\theta Z}\right\} = pe^{-\theta Z} + qe^{\theta Z}. \tag{3.2}$$

Consider $X(t)$ as the total displacement after $n = \frac{t}{\tau}$ steps. Since displacements in different time steps are independent, we will have:

$$E\{X(t)\} = (t/\tau)(p-q)\Delta, \tag{3.3}$$

$$Var\{X(t)\} = (t/\tau)4pq\Delta^2. \tag{3.4}$$

We wish to let $\Delta \to 0$ and $\tau \to 0$ in a sense that we get a meaningful result. In other words, say we want the displacement process to have a mean μt and variance $\sigma^2 t$ (based on (3.3) and (3.4), mean and variance are time dependent). Therefore, it is required that Δ and τ tend to zero in such a way that:

$$(p-q)\Delta/\tau \to \mu, \tag{3.5}$$

$$4pq\Delta^2/\tau \to \sigma^2. \tag{3.6}$$

This will be satisfied if:

$$\Delta = \sigma\sqrt{\tau}, \tag{3.7}$$

$$p = \frac{1}{2}\left(1 + \frac{\mu\sqrt{\tau}}{\sigma}\right), \tag{3.8}$$

$$q = \frac{1}{2}\left(1 - \frac{\mu\sqrt{\tau}}{\sigma}\right). \tag{3.9}$$

Based on (3.7), the change in position ($\Delta = \Delta x$) in a small time interval ($\tau = \Delta t$) is of the order of magnitude $(\Delta t)^{1/2}$.

Now, we derive the equation for probability distribution in continuous time and space condition. The forward Kolmogrov equation for the Brownian motion is:

$$p_{jk}^{(n)} = p_{jk-1}^{(n-1)}p + p_{jk+1}^{(n-1)}q, \tag{3.10}$$

where, $p_{jk}^{(n)}$ is the probability that a diffusing particle at the position $j\Delta x$ gets to the position $k\Delta x$ after n steps.

Letting $p(x_0, x; t)\Delta x$ denote the probability that the particle is at x at time t, given that it was at x_0 at t=0, we have $x_0 = j\Delta x$, $x = k\Delta x$, and $t = n\Delta t$. Also, (3.10) will become:

$$p(x_0, x; t) = pp(x_0, x - \Delta x; t - \Delta t) + qp(x_0, x + \Delta x; t - \Delta t). \tag{3.11}$$

Suppose $p(x_0, x; t)$ could be differentiated a suitable number of times. Therefore, we can write the Taylor series as:

$$p(x_0, x+\Delta x; t-\Delta t) = p(x_0, x; t) - \Delta t\frac{\partial p}{\partial t} + \Delta x\frac{\partial p}{\partial x} + \frac{1}{2}(\Delta x)^2\frac{\partial^2 p}{\partial x^2} + \cdots . \tag{3.12}$$

Expanding (3.11) in this way, and using (3.7), (3.8), and (3.9), and letting $\Delta t \to 0$, we will obtain:

$$\frac{1}{2}\sigma^2\frac{\partial^2}{\partial x^2}p(x_0, x; t) - \mu\frac{\partial}{\partial x}p(x_0, x; t) = \frac{\partial}{\partial t}p(x_0, x; t). \tag{3.13}$$

It is a partial differential equation of the second order in x and first order in t[1].

For the case where the particle has no biased movement, $p = q = \frac{1}{2}$. So, $\mu = 0$, and (3.13) will become:

$$\frac{1}{2}\sigma^2\frac{\partial^2}{\partial x^2}p(x_0, x; t) = \frac{\partial}{\partial t}p(x_0, x; t). \tag{3.14}$$

Solving (3.14) needs one initial and two boundary conditions. We already have the initial condition:

$$p(x, 0) = \delta(x - x_0). \tag{3.15}$$

Two boundary conditions are needed. Considering that $p(x; t)$ is a p.d.f., and also that the particle will never reach infinity, we will have:

$$\int p(x, t)dx = 1, \tag{3.16}$$

$$p(\infty, t) = 0. \tag{3.17}$$

Under these conditions, the solution for (3.14) will be:

$$p(x, t) = \frac{1}{\sqrt{2\pi\sigma^2 t}}e^{-(x-x_0)^2/2\sigma^2 t}. \tag{3.18}$$

We note that biological texts use D instead of σ, and call it diffusion coefficient.

[1]Considering (3.7), Δx is of the order of magnitude $(\Delta t)^{1/2}$. So, $(\Delta x)^2$ should be considered, as well.

3.2 Jump Diffusion Process

Brownian motion is considered as the basic model illustrating molecular communication. However, advanced molecular communication methods cannot be modeled using simple Brownian motion. Molecular communication using filaments in free space assumes that a number of filaments are attached to receivers. A released information molecule diffuses through the medium and if it reaches a filament, the molecule will attach to the filament, and moves along it to reach the receiver. Obviously, molecular propagation in this method of communication is not purely based on diffusion. This process can be considered as a Brownian motion with discontinuities. The mathematical model illustrating this type of movement is called jump diffusion process.

A jump diffusion process is defined as a Brownian motion with discontinuities (or jumps). Mathematically, it is of the form:

$$X_t = \sigma B(t) + \mu t + \sum_{i=1}^{N(t)} J_i, \tag{3.19}$$

where, $B(t)$ is Brownian motion with zero drift and variance 1, σ is the square root of variance of the process, μ is the drift of the process, $N(t)$ is a Poisson process with rate λ, and jump sizes $\{J_i, i = 1, 2, ...\}$ are independent identically distributed random variables. Without loss of generality, we assume $\sigma = 1$, and considering the scenario, $\mu = 0$. Also, we assume $B(t)$, $N(t)$, and random variables $\{J_i, i = 1, 2, ...\}$ are independent. It should be noted that since $B(t)$ is a Markov process, $N(t)$ has Poisson distribution, and J_is are independent, X_t is also a Markov process.

Unfortunately, jump diffusion processes have not been investigated thoroughly, yet. Specifically, if jump sizes are not independent double exponential random variables (one exponential random variable if the jump is in the positive direction, and another exponential random variable if the jump is in the negative direction), formulating the process will be complex [48]. Some research works have considered jump distributions other than double exponential, such as hyper-exponential [49], but considering an arbitrary jump size makes it very complex. However, we can use approximation methods to find the position distribution of a particle moving based on this type of process. In the rest of this chapter, we will discuss an approximation method, which uses discrete time Markov chains, to model jump diffusion process.

The method will be used to model propagation process in molecular communication using filaments in free space.

3.3 DTMC Approximation

In this section, we discuss an approximation method for jump diffusion processes based on discrete time Markov chains. We start with approximating a one dimensional Brownian motion and then extend the model for a two dimensional process. Finally, we modify the Markov chain to model a jump diffusion process.

3.3.1 Brownian motion approximation

In this section, we introduce a DTMC approximation for free Brownian motion based on [50]. Assume D is 1 (standard Brownian motion). We will relax this assumption at the end of this section. Also, assume a one dimensional space, which is bounded to X_1 and X_2 ($X_1 < X_2$). Consider m as a large number (the larger the m the more accurate the model. For a given error, a sample scenario can be considered to find minimum m which satisfies the error). We divide the one dimension space into m equal length intervals, each with length of $\Delta x = \frac{X_2 - X_1}{m}$ (discrete space)[2]. Also, we choose $\Delta t = \frac{1}{\Delta x^2}$. Now, considering (3.18), it is straightforward to show that probability distribution of the displacement of a diffusing particle, X, in Δt can be calculated as:

$$P(X = k\Delta x) = \begin{cases} \frac{C^{-1}}{\sqrt{2\pi}} exp(\frac{-k^2}{2}) & k \neq 0 \\ \frac{C^{-1}}{\sqrt{2\pi}} \sum_{l \neq 0} (l^2 - 1) exp(-\frac{l^2}{2}) & k = 0, \end{cases} \tag{3.20}$$

where C is a normalizer factor and equal to:

$$C = \frac{1}{\sqrt{2\pi}} \sum_{l \neq 0} (l^2) exp(-\frac{l^2}{2}). \tag{3.21}$$

Now, consider a Markov chain whose states are the spatial intervals introduced earlier (Δx) and the transition probabilities are defined based on

[2]Division of x axis in this section should not be confused with what was done in Section 3.1, where $\Delta x \to 0$. In this section, m can be any integer.

(3.20). Therefore, the entries of the corresponding transition matrix of the Markov chain, T, are:

$$T_{ij} = P(X_{t+1} = j\Delta x | X_t = i\Delta x), \quad i, j = 1, 2, ..., m, \tag{3.22}$$

where, X_t is the state of the Markov chain at time t. This probability can be calculated by putting $k = j - i$ in (3.20).

It is shown in [50] that if:

$$W(t) = state\ of\ the\ Markov\ chain\ at\ t, \tag{3.23}$$

then:

$$W(t) \to B(t), \quad as \quad \Delta x \to 0, \tag{3.24}$$

where, $B(t)$ is standard Brownian motion. In other words, the Markov chain approximates the position of a diffusing particle at $t = n\Delta t, n = 0, 1, ...$ It is worth mentioning that since the probability distribution in (3.18) is not a function of x (it is a function of Δx), the transition probabilities presented for the Markov chain are not a function of X_t or X_{t+1}. They are only a function of $X_{t+1} - X_t$.

T is the transition matrix of a discrete PH-type distribution representing boundary crossing probability for Brownian motion. In other words, considering α as the initial distribution for the position of a particle, boundary crossing probability distribution of the Brownian motion is equal to the absorbing time distribution of the PH-type distribution (T, α).

In order to be comprehensive, we extend the model to a two dimensional space. We build a Markov chain with state space (X, Y) where X defines the x component and Y defines the y component of the position of a particle. Since x and y components of a Brownian motion are independent and the transition probabilities for both components follow (3.20), the transition matrix of the Markov chain will be:

$$\hat{T} = T \otimes T, \tag{3.25}$$

where, T is defined in (3.22) and $\otimes$ is the Kronecker product, which is defined as follows. If A is a $m \times n$ matrix with a_{ij} as the entry at row i and column j and B is a $p \times q$ matrix, the Kronecker product of A and B is defined as:

$$A \otimes B = \begin{bmatrix} a_{11}B & \dots & a_{1n}B \\ \vdots & \ddots & \vdots \\ a_{m1}B & \dots & a_{mn}B \end{bmatrix}. \tag{3.26}$$

Finally, what if $D \neq 1$? It is stated in [50] that one can still assume $D = 1$, and modify the boundary of the channel instead. If R stands for the boundary of the actual channel, the boundary of the modified channel will be $\frac{1}{\sqrt{D}}R$.

3.3.2 Jump diffusion process approximation

Consider the one dimensional Brownian motion introduced in Section 3.3.1. In order to use the approximation method introduced in Section 3.3.1 for jump diffusion processes, we discretize time. Consequently, inter-jump intervals have geometric distribution (with parameter $\lambda\Delta t$) and jumps happen only at the end of a time unit. Also, assume:

$$P(J = k\Delta x) = J(k). \tag{3.27}$$

Considering spatial intervals as the states of a Markov chain, the entries of the corresponding transition matrix, S, are as follows:

$$S_{ij} = (1 - \lambda\Delta t)T_{ij} + \lambda\Delta t J(j - i), \tag{3.28}$$

where, T is the transition matrix introduced in Section 3.3.1.

In order to be comprehensive, we extend the model to a two dimensional space. We assume the x and y components of a jump diffusion process are independent. It should be noted that we are proposing a stochastic model. Therefore, it is not necessary to follow the exact movement of a particle. However, the model should statistically match the movement. Therefore, it is valid to assume x and y components of jumps are independent given that the distributions match the distributions in the scenario. To be more specific, jumps in the x and y components might not happen at the same time slot, but looking at the whole process, the jumps on the x and y components match stochastically. Therefore, the one dimensional approximation can be extended to approximate a two dimensional jump diffusion process as explained in Section 3.3.1. The transition matrix of the resulting Markov chain, $\hat{S}$, will be:

$$\hat{S} = S \otimes S, \tag{3.29}$$

where, S is given in (3.28).

3.4 Molecular communication using filaments

The most realistic scenario considered for molecular communication using filaments is called communication in free space. It assumes a fixed number of filaments are attached to each receiver. A released information molecule diffuses through the medium and in case it reaches a filament it will attach to the filament, and moves along it to reach the receiver. However, it is shown that this scenario has a poor performance in terms of the coverage range of a transmitted signal, delay, and fairness. Borrowing the idea from wireless communication, we introduce relay nano-machines employment as a technique to overcome these drawbacks. Relay nano-machines will enlarge the coverage of a nano-network. In this section, we use Markov chain approximation for jump diffusion processes to model the propagation process in this scenario.

Consider a channel with one transmitter which releases one information molecule already attached to a molecular motor. To elaborate on the performance improvements of the proposed technique, we consider a bounded two dimensional channel where the transmitter is at the middle of it (equal distance to the boundaries). Also, the two boundaries on the two sides of the channel are receivers. If a motor hits the other boundaries it will be reflected. Also, all the nodes have relaying capability. Assume an average of N nano-relays are distributed in the channel based on a Poisson point process, and M filaments are attached to each of them. The orientations of all the filaments attached to a nano-relay are uniformly distributed between 0 and 2π (with respect to the x axis) except for one filament which is oriented towards the closest receiver (if a nano-relay has equal distances to receivers, we pick one receiver at random as the closest receiver). If a nano-relay receives a motor, instead of removing the motor, it will put the motor on this filament. This will guide the motor towards the closest receiver.

We have assumed nano-relays are capable of distinguishing a filament, and also, putting a motor on a specific filament. An example for the former assumption (distinguishing a filament) is the transmigration across endothelial cells (cells that line the interior surface of blood vessels) [51, 52]. The nucleoid of these cells receives cargoes from filaments attached to one side of it and picks one of the filaments leading to a blood vessel to put the motor on, and consequently, sends the cargo into blood stream. In addition to this example, a practical technique is using concentration gradient. Assuming that the receivers emit a specific type of molecules, the concentration of

the molecule is higher on the receiver side and it can be sensed by nano-relays. We propose a high level model in this paper and assume this process is performed in an ideal manner. The latter assumption can be achieved if nano-relays release motors and the cargo at a vicinity of the intended filaments. The higher the concentration of motors at the vicinity of the filament is, the higher the probability of the cargo attaching to a motor and the motor attaching to the filaments. In this paper, for tractability reasons, we assume that the concentration of motors is high enough and probability of attaching to the filament is 1.

There are different types of molecular motors. Attaching to a filament, a molecular motor may move towards the +ve end or the -ve end of the filament, depending on the type of the motor. For example, Myosin 6 move towards -ve end of a filament and most other Myosins move toward the +ve end [29]. Assume each nano-relay is located either on the +ve end (R+ topology) or on the -ve end (R- topology) of all of the filaments attached to it. If a nano-relay in an R+ topology receives a motor, since the nano-relay is on the +ve side of all the filaments attached to it, the motor has moved towards the +ve end of the filament. Having received a motor, the nano-relay should bond the received information molecule to a motor and put it on the filament directed towards the receiver. However, this time the motor is supposed to move towards the -ve end of the filament (away from the nano-relay). Since the received motor moves towards the +ve end of a filament, the nano-relay should use a different type of motor which moves towards the -ve end of a filament. We assume each nano-relay stores as many motors as needed, and it is capable of breaking the bond between an information molecule and a motor, and making a new one between the information molecule and a new motor. A comprehensive discussion on how these processes could be done and what are the necessary conditions on the information molecules and the motors can be found at [53]. Half of the nano-relays have R+ and the other half have R- configurations in the scenario .

Consider a motor which moves towards -ve end of a filament. Being released from the transmitter, the motor diffuses through the medium and in case it reaches a filament, it will attach to the filament. If the motor attaches to a filament belonging to a nano-relay in an R- topology, the motor will start moving towards the nano-relay. However, if the motor attaches to a filament in an R+ topology, it will move towards the -ve end of the filament and away from the nano-relay. These two scenarios are treated separately in the model.

Without loss of generality, we assume filaments are straight. If the fila-

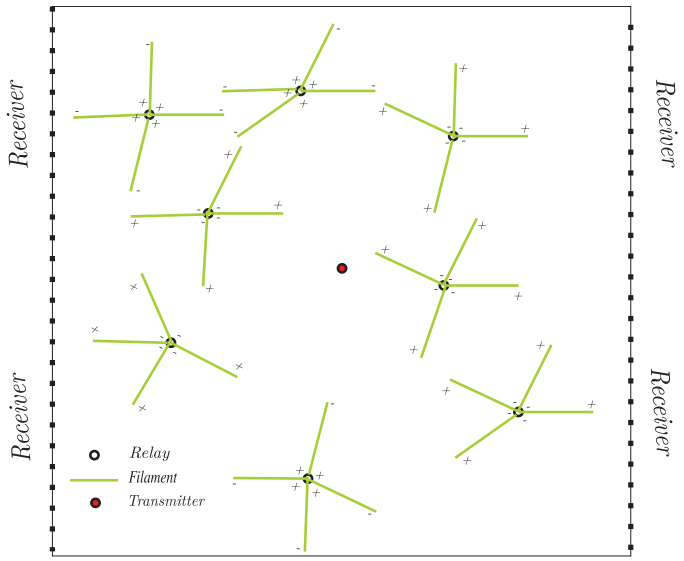

Figure 3.1: A sample scenario. The transmitter is in the middle of the channel and the two right and left sides of the channel are considered as receivers.

ments are not straight, the jump distribution would change. However, the same approach can be applied to find the model for molecular propagation. Also, it is assumed that filaments are shorter than the average distance between neighbor nano-relays and longer than half the distance. If filaments are shorter diffusion will be the dominant process for propagation and therefore, using the proposed technique is not advantageous. Figure 3.2 shows a comparison for the scenario considered in this thesis between filaments' length of $10\mu m$ and $5\mu m$ and free Brownian motion (in the considered scenario, average distance between nano-relays is $11.2\mu m$). It can be seen in the figure that performance of the former scenario is close to performance of free diffusion in terms of delay. On the other hand, if filaments are longer than the range, there will be several crossovers. Since the model proposed in this thesis does not consider crossovers, the results for such a scenario will not be accurate. Additionally, we assume all the filaments have the same length. Future works can relax these assumptions and make the model more general. Figure 3.1 shows the scenario for eight nano-relays, i.e. $N = 8$, in the channel with four filaments, i.e. $M = 4$.

As long as a released motor is not attached to a filament, it freely diffuses through the medium. If it reaches a filament, depending on its type it will

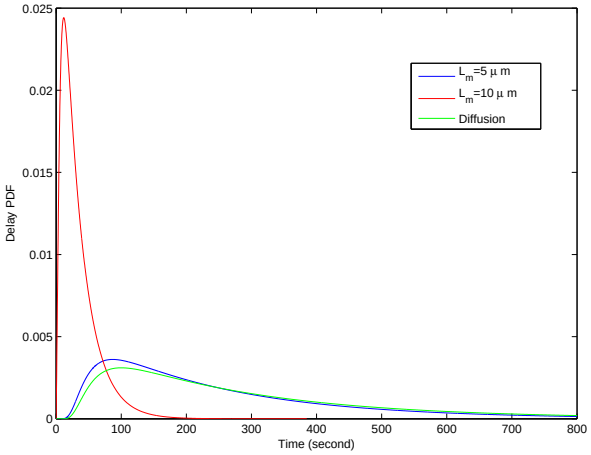

Figure 3.2: Comparison between three scenarios: filaments are long, filaments are short, and free diffusion.

start walking towards the nano-relay or the other end of the filament. Either way, the motor will reach the end of a filament after some time and diffuse again. So, if we look at the whole process of a motor's movement in the medium, it is a Brownian motion with discontinuities. In other words, the attaching and detaching processes will cause discontinuities in the Brownian motion and jumps in the position of the motor. This leads to the idea of using jump diffusion processes.

We note that not all released motors reach a filament. However, considering that the length of filaments are not too short (compared to the average distance between nano-relays), it happens with a high probability. Also, the proposed model is probabilistic. Therefore, it does not assume that all information molecules attach to filaments with probability 1. Inter-jump intervals and jump sizes are the two random variables that should be known to define a jump diffusion process. In this regard, we first discuss that it is reasonable to assume that the distribution of the inter-jump times is exponential, and then, find the parameter of the distribution. Next, we calculate the jump size probability distribution.

A motor which is not attached to a filament diffuses through the medium. Considering the independent increments property of diffusion, and also the assumption that nano-relays are distributed based on a Poisson point pro-

cess, the remaining time to the next attachment is independent of the time passed since the last attachment of a diffusing motor. Therefore, the time interval between two consecutive attachments to filaments has an exponential distribution.

In order to find the rate of the inter-jump process, we use a known formula. It is known that the average time for a diffusing particle to pass a circle of radius Δr in a two dimensional space for the first time is [54]:

$$t_{avg} = \frac{1}{2D}(\Delta r)^2, \tag{3.30}$$

where, D is the diffusion coefficient of the medium. Therefore, if d_{avg} is the average distance a motor diffuses between two consecutive attachments to filaments, the average inter-attach interval, or equivalently inter-jump time for a motor is:

$$t_{avg} = \frac{1}{2D}{d_{avg}}^2, \tag{3.31}$$

and consequently, the rate of the inter-jump process will be:

$$\lambda = \frac{1}{t_{avg}} = \frac{2D}{{d_{avg}}^2}. \tag{3.32}$$

We need to find d_{avg}. Since d_{avg} is the average distance, we consider a symmetric channel. We divide the channel into N equal squares (N is the number of nano-relays) and consider one nano-relay at the middle of each square (a symmetric channel in terms of the position of nano-relays). For an arbitrary nano-relay, named A, the four nano-relays located on its right, left, up, and down consist the first set of neighboring nano-relays. The nano-relays between each two members of the first set consist the second set, and so on. Figure 3.3 illustrates a sample topology. We assume that a motor detached from A will attach to a filament belonging to neighboring nano-relays of A. We find the number of sets of neighbors that should be considered in the model and also the probabilities of binding to each set of neighbors. As we will show, the average distance between two nano-relays that a motor attaches to their filaments consecutively is close to the average distance between A and the set of its first, second, and third closest neighboring nano-relays. Therefore, we assume that a motor detached from nano-relay A will attach to a filament belonging to the set of first, second, or third closest neighboring nano-relays of A. To derive the binding probabilities, we present simulation results for the distribution of the distance between two nano-relays that a

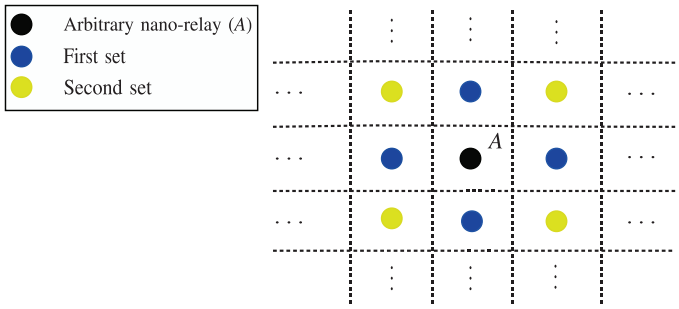

Figure 3.3: Illustrating the first and second sets of neighbors for an arbitrary nano-relay named A.

motor attaches to their filaments consecutively. We consider a two dimensional channel ($100 \times 100\mu m$). The size of the channel is chosen in a way to ensure that a released motor attaches to at least one filament before reaching a receiver and also diffuses after detaching from the filament. Therefore, the channel dimensions are much longer than both the average distance a motor moves between two consecutive attachments, which is $14.10\mu m$, (to ensure motors attach to at least one filament), and the length of filaments (to ensure motors are not received immediately after detaching from filaments). The rate of the Poisson point process for nano-relays distribution is 8×10^9. The simulation results are presented for two length of filaments: $5\mu m$ and $10\mu m$ to ensure the generality of the results. As shown in Figure 3.4, the distribution of the distance between two nano-relays that a motor attaches to their filaments consecutively is close to uniform distribution. Therefore, we assume the probability of binding to the filaments of the three sets of neighboring nano-relays is the same (equal to $\frac{1}{3}$).

Considering the above mentioned setting, $d_{avg,1}$, $d_{avg,2}$, and $d_{avg,3}$ are the average distances of nano-relay A to another nano-relay belonging to the set of A's first, second, and third closest neighbors, respectively. The average distance between A and another nano-relay belonging to the set of A's closest neighbors is:

$$d_{avg,1} = \sqrt{\frac{XY}{N}}, \tag{3.33}$$

where, X and Y are the width and length of the channel. Similarly, the

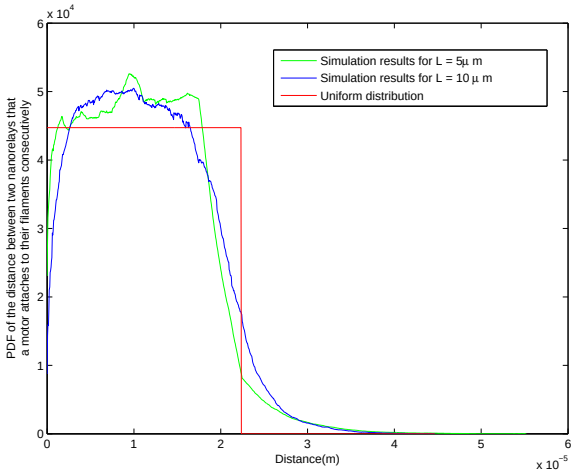

Figure 3.4: Distribution of the distance between two nano-relays that a motor attaches to their filaments consecutively for different filament lengths.

average distance to the set of second and third closest neighbors are:

$$d_{avg,2} = \sqrt{2}d_{avg,1}, d_{avg,3} = 2d_{avg,1}. \tag{3.34}$$

Using this technique, for the scenario in which filaments' length is $10\mu m$ the average distance between two nano-relays that a motor attaches to their filaments consecutively is $14.10\mu m$ and $16.14\mu m$, based on simulation and analytic results, respectively. The error is 12.5%, which is negligible. For the scenario in which filaments' length is $5\mu m$ the average distance based on analytic result is the same, and based on the simulation results is $13.66\mu m$. The error is 14.3%, which is not as good as the other scenario, but still not huge.

If an emitted motor attaches to one of the first neighbors, based on Figure 3.5 the distance it should diffuse is:

$$d_1 = (d_{avg,1} - L)sin(\frac{\pi}{M}), \tag{3.35}$$

where, L is the length of a filament, and $\frac{2\pi}{M}$ is the average angle between two adjacent filaments attached to a nano-relay.

To find the average distance a motor diffuses to attach to a filament belonging to the second or third neighbors, we assume the motor attaches to

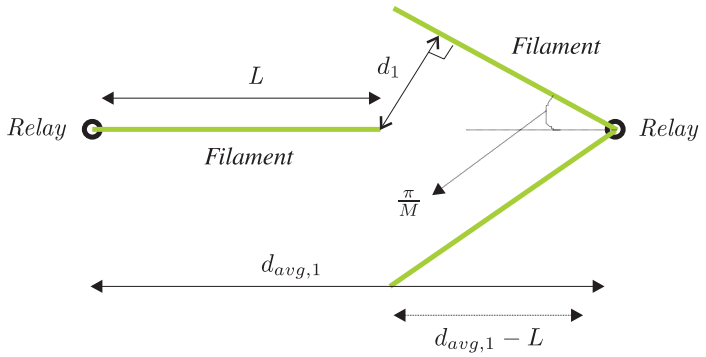

Figure 3.5: The average distance a motor should diffuse to reach a nano-relay belonging to the set of the nearest neighbors.

the middle of the filament. Nano-relays are distributed based on a PPP, and therefore, they are uniformly distributed in the channel. Since the average distance between A and another nano-relay belonging to the set of its second or third neighbors is longer than the length of filaments, the motor should diffuse throught the channel to reach the next filament. Consequently, the probability distribution of the position a motor attaches to a filament belonging to the next nano-relay is defined based on a Brownian motion. Since the direction of each step in Brownian motion is picked based on a uniform distribution, the distribution is approximately uniform over the length of the filament. Results shown in Figure 3.6 validates this assumption. Figure 3.6 compares the probability distribution for the position where a motor attaches to a filament based on simulations (blue) with a uniform distribution for the same interval (red). Based on this figure, the probability distribution is very close to uniform. The probability distribution deviates from the uniform distribution for up to 5.8%. Considering this assumption and Figure 3.7, the average distance a motor should diffuse is:

$$d_i = \sqrt{(d_{avg,i} - \frac{L}{2})^2 + \frac{L}{2}^2 - 2(d_{avg,i} - \frac{L}{2})\frac{L}{2}cos(\frac{\pi}{M})},$$
$$i = 2, 3. \tag{3.36}$$

Therefore, the average distance a motor should diffuse to reach a filament is:

$$D_{avg1} = \frac{d_1 + d_2 + d_3}{3}. \tag{3.37}$$

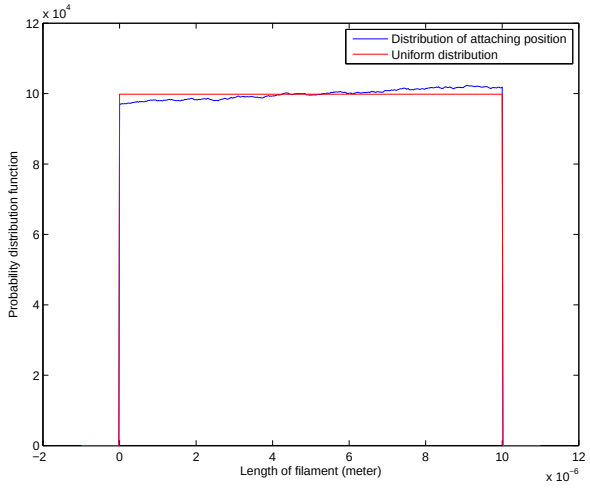

Figure 3.6: Probability distribution of the position a motor attaches to the next filament and a uniform distribution.

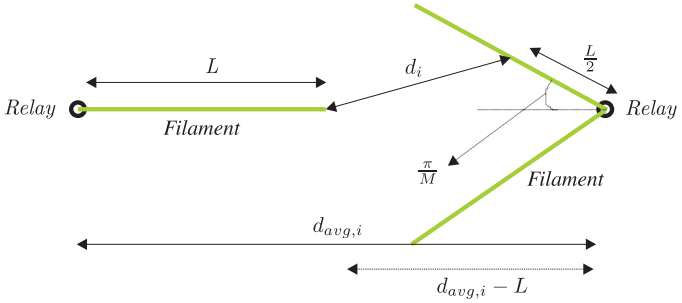

Figure 3.7: The average distance a motor should diffuse to reach a nano-relay belonging to the set of the second or third nearest neighbors.

It is worth noting that we assumed the orientation of at least one filament of each nano-relay is fixed towards the closest receiver. Let us call such filament M_d. If polarity of a motor is in match with the filament it attaches to, the motor will detach from M_d filament of the nano-relay. In this case, the probability that the motor attaches to M_d of any of the neighbor nano-relays is low since M_d is the furthest filament and the motor should go around a nano-relay to reach it. This will modify (3.35) and (3.36) by changing M to $M-1$. We call the average distance calculated for this scenario D_{avg2}. However, if the polarity of an attached motor is not in match with the filament

it is attached to, (3.35) and (3.36) will remain as they are. Since the number of nano-relays in R+ and R- topology are equal and they are distributed in the channel uniformly, the average distance a motor should diffuse between two consecutive attachments to filaments is:

$$D_{avg} = \frac{D_{avg1} + D_{avg2}}{2}. \tag{3.38}$$

Next, we derive the jump size probability distribution. Since it is more understandable, we find the distribution of the jump process, shown by J, in the discrete space defined for the DTMC approximation. In what follows, we calculate the jump size on the x axis. First, consider the case where the polarities of a motor and the filament do not match (the motor does not move towards the nano-relay). We divide this scenario into two parts: a motor attached to a filament other than M_d, and a motor attached to M_d. Starting with the former one, Figure 3.8 shows an arbitrary scenario. Δx is the spatial step in the DTMC approximation method. Considering Figure 3.8, if the motor attaches to the region defined by r_1, when the motor finishes moving on the filament, the displacement of the motor (Δd) will be equal to one unit. Therefore, the displacement of a motor due to its movement on a filament is equal to one unit with probability:

$$P(\Delta d = 1) = P(motor\ attaches\ to\ r_1)P(\theta_1 < \theta < \theta_2), \tag{3.39}$$

where, θ_1 and θ_2 are shown in Figure 3.8. Filaments of different nano-relays make different angles with the x axis. Different angles lead to different motor displacements on the x axis caused by moving along the filament. θ_1 and θ_2 define the range that lead to a displacement of $j\Delta x$. Assuming that a motor attaches to different positions on a filament with equal probability, we have:

$$P(motor\ attaches\ to\ r_1) = \frac{r_1}{L}. \tag{3.40}$$

r_1 is the portion of a filament located $(j-1)\Delta x$ away from the nano-relay. Swiping θ from θ_1 to θ_2, r_1 will change. However, choosing a small enough Δx, the change is small enough to be ignored. Also, since the angle between a filament and the x axis is uniformly distributed, we have:

$$P(\theta_1 < \theta < \theta_2) = \frac{\theta_2 - \theta_1}{2\pi}, \tag{3.41}$$

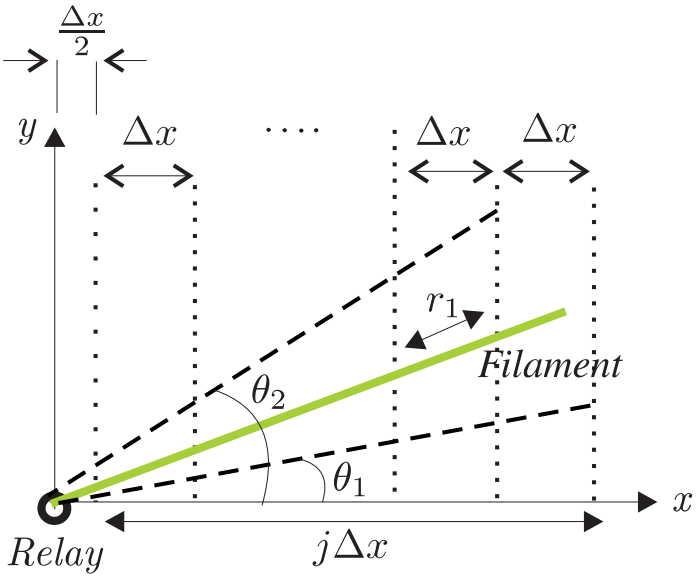

Figure 3.8: Jump size of one, for an arbitrary position of a filament.

where:

$$\theta_1 = acos((\frac{\Delta x}{2} + j\Delta x)/L), \tag{3.42}$$

$$\theta_2 = acos((\frac{\Delta x}{2} + (j-1)\Delta x)/L). \tag{3.43}$$

A similar approach can be used to derive the probability of one unit displacement for all possible intervals of θ, and sum them to find the probability of jump size equal to one, if a motor attaches to a filament other than M_d. Similarly, the probability distribution of different jump sizes can be found. We call this probability distribution J_1.

What if a motor attaches to an M_d? The only difference will be in θ, since for $M_d, \theta = 0$. Having defined θ, the same approach as before could be used to find jump size probability distribution for a motor that attaches to an M_d. We call this probability distribution J_2.

Assuming a motor attaches to the filaments attached to a nano-relay with equal probability, the probability distribution of the jump size for the case where the polarity of a motor and the filament it is attached to are not in match is:

$$J_n = \frac{M-1}{M} J_1 + \frac{1}{M} J_2. \tag{3.44}$$

Clearly, the assumption of equal probability for a motor attaching to the filaments of a nano-relay is not exact. But, as we will see in the results, this will not affect the model much.

Figure 3.9(a) shows the probability distribution function of J_n for a motor that attached to a nano-relay with $10\mu m$ long filaments and M_d of the nano-relay is directed towards the right end receiver.

We assume the jump process along x and y axes are independent. Considering the model is a probabilistic analysis of motors propagation, this is a reasonable assumption. Therefore, a similar method is used to find the jump distribution on the y axis.

Now, if the polarity of a motor and the filament are in match, the motor starts walking towards the nano-relay. Being received, a motor is put on the filament directed towards the closest receiver (M_d) and moves away. We divide this relocation of the motor into two parts: the relocation before it reaches the nano-relay, and the relocation after it is put on M_d. The probability distribution for the first part can be derived using a similar approach as discussed before. The second part of the relocation is deterministic. Since a motor received by a nano-relay will be put on M_d and the receivers are the two side boundaries of the channel, the second part of the relocation will be equal to L on the x axis, and 0 on the y axis. We call this probability distribution J_p. Figure 3.9(b) shows the probability distribution function of the jump size of a motor whose polarity is in match with the filament it is attached to, on the x axis. In Figure 3.9(b), the length of the filament is $10\mu m$ and the M_d of the considered nano-relay is directed towards the right end receiver. Considering nano-relays are distributed uniformly between R+ and R- topology, the overall jump size distribution is:

$$J = \begin{cases} J_n & \text{with probability } \frac{1}{2} \\ J_p & \text{with probability } \frac{1}{2}. \end{cases} \tag{3.45}$$

Having calculated all the needed probabilities, we build the transition matrix of the molecular propagation model for the molecular communication via filaments using nano-relays based on the matrix structure defined in Section 3.3. However, one point is left. We note that the average speed assumed for a moving motor along a filament is $v = 10\frac{\mu m}{s}$. Therefore, it takes $\frac{r}{v}$ seconds for a motor to move r meters on a filament. We should modify the proposed model to capture this issue, since in the model each jump takes one unit of time (Δt), where based on the DTMC approximation method discussed in

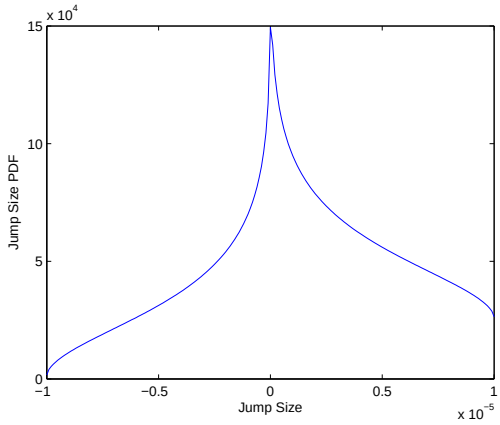

(a) Polarities of the motor and the filament do not match

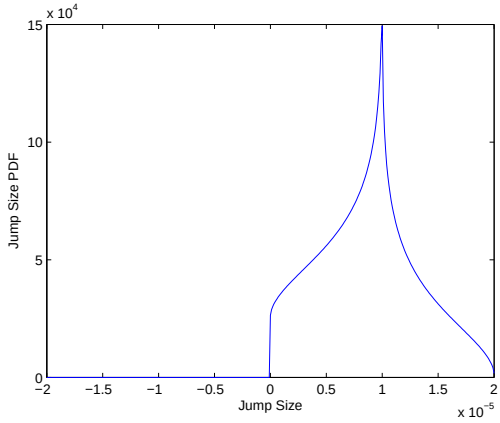

(b) Polarites of the motor and the filament match

Figure 3.9: Probability distribution function for jump size (length of filaments are $10\mu m$).

Section 3.3.1, is equal to:

$$\Delta t = \Delta x^2. \tag{3.46}$$

Consider Δt_p equal to the average time a motor is attached to a filament (having calculated J, and assuming v is known, it is straightforward to find Δt_p), and choose Δx_p based on (3.46). Defining Δx_p as the spatial step, the average time a motor is attached to a filament will be equal to the time unit of the model, and the issue of a mismatch between the time unit of the model

and the time interval a motor is attached to a filament is solved.

Having developed the model based on a DTMC approximation for a jump diffusion process, we discuss how the model can be used to derive a phase type distribution representing molecular delay in molecular communication via filaments using nano-relays. Consider T_{markov} as the transition matrix of the Markov chain modeling molecular propagation. Clearly, the Markov chain defines the position of a motor as long as its position is between the boundaries. Assume a simple case of one dimensional channel divided into five intervals (states). Transition matrix of the Markov chain standing for molecular propagation in the channel is:

$$T_{markov} = \begin{bmatrix} 1 & 0 & 0 & 0 & 0 \\ p^A_{2,1} & p_0 & p_1 & p_2 & p^A_{2,5} \\ p^A_{3,1} & p_{-1} & p_0 & p_1 & p^A_{3,5} \\ p^A_{4,1} & p_{-2} & p_{-1} & p_0 & p^A_{4,5} \\ 0 & 0 & 0 & 0 & 1 \end{bmatrix}, \tag{3.47}$$

where, $p_r = S_{i,i+r}, r = -2, -1, 0, 1, 2$ ($S_{i,j}$ defined in (3.28)), and $p^A_{i,1}$ is the probability of absorbing to state 1 from state i, calculated as:

$$p^A_{i,1} = (1 - \lambda\Delta t)\left(\frac{1}{2} - \frac{1}{2}q_0 - \sum_{r=1}^{i-2} q_r\right) + \lambda\Delta t \sum_{r=i-1}^{J_{max}} J, \tag{3.48}$$

$p^A_{i,5}$ is the probability of absorbing to state 5 from state i, calculated as:

$$p^A_{i,5} = (1 - \lambda\Delta t)\left(\frac{1}{2} - \frac{1}{2}q_0 - \sum_{r=1}^{i} q_r\right) + \lambda\Delta t \sum_{r=i+1}^{J_{max}} J, \tag{3.49}$$

where, $q_r = P(X = r\Delta x)$ defined in (3.20) , and J_{max} is the maximum jump size.

Molecular delay is the time distribution for the Markov chain to absorb to any of the absorbing states. Therefore, if we consider T_{mp}, t^0, and α_{mp} as:

$$T_{mp} = \begin{bmatrix} p_0 & p_1 & p_2 \\ p_{-1} & p_0 & p_1 \\ p_{-2} & p_{-1} & p_0 \end{bmatrix}, \tag{3.50}$$

$$t^0 = \begin{bmatrix} p^A_{2,1} & p^A_{2,5} \\ p^A_{3,1} & p^A_{3,5} \\ p^A_{4,1} & p^A_{4,5} \end{bmatrix} \times \begin{bmatrix} 1 \\ 1 \end{bmatrix}, \tag{3.51}$$

$$\alpha_{mp} = \begin{bmatrix} a_2 & a_3 & a_4 \end{bmatrix}, \tag{3.52}$$

where, α_{mp} is the distribution of the initial state (position) of a motor (we assume initial position of a motor is not at any of the absorbing states), (α_{mp}, T_{mp}) will be a phase type distribution representing time to absorption, or delay, of the motor. It should be noted that since PH distribution is defined as time until absorption of a Markov chain with only one absorbing state, we defined t^0 as the way shown at (3.51). More specifically, we considered both absorbing states as one state. This is valid because in our scenario, it is not important that the original Markov chain has absorbed to which of the absorbing states.

Considering the above explanation, the delay distribution of the motor is:

$$\begin{aligned} p(k) &= p\{delay = k \ units \ of \ time\} \\ &= \alpha_{mp}(T_{mp})^{k-1}t^0. \end{aligned} \tag{3.53}$$

3.5 Stationary distribution of molecules in nano-communication via filaments

In this section, we use the model proposed in Section 3.4 to find the stationary distribution of information molecules in the channel. We modify the scenario to fit this goal and also improve the model.

The idea of deploying nano-relays is used in the scenario shown in Figure 3.10 to guide motors towards the desired region. If a motor reaches a filament, it will attach to the filament and move towards the nano-relay. Then, the nano-relay will put the motor on the filament directed towards the desired region, and therefore, guide the motor.

It is assumed nano-relays are distributed based on a Poisson point process. Also, the number of filaments attached to nano-relays is the same for all nano-relays, and at least one filament attached to each nano-relay is directed towards the desired region (not necessarily exactly pointing at the desired region. This is an important improvement to the model proposed in Section 3.4). In regard to the filaments, they are all the same length, and other than the one directed towards the desired region, the angle between them and the x axis is uniformly distributed.

We divide the whole space into three regions: desired region, undesired region, and transient region. The desired region is the region which we are

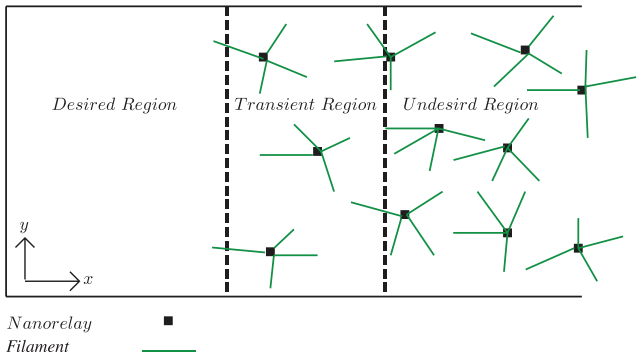

Figure 3.10: The scenario.

interested to keep the molecules in. The undesired region is the region far from the boundary of the desired region where molecules sense a homogeneous region in terms of nano-relays distribution. The region in between is called transient region. In Section 3.4, it is stated that if filaments attached to nano-relays are neither too short nor too long, a molecule detaching from an arbitrary nano-relay, called A, will attach to a filament belonging to the set of the first, second, or third layers of neighbors of A (also stated in Section 3.4). Therefore, as long as a nano-relay has three layers of neighbors around it, it could be assumed that nano-relays are distributed in the whole channel based on the desired Poisson point process. Considering this result, if d_{nn} is the average distance between two adjacent nano-relays, nano-relays located $2d_{nn}$, or further, away from the boundary of the desired region have three layers of neighbors, and to molecules detaching from filaments belonging to them the channel is homogeneous. Based on the above discussion, length of the transient region is $2d_{nn}$.

Molecular propagation in three regions of Figure 3.10 are not similar. In the desired region, it is pure Brownian motion and the first model discussed in Section 3.3.1 is a good approximation for the propagation in this region. Also, molecular propagation in the transient and undesired regions can be considered as jump diffusion processes. Based on the detailed discussions in Section 3.4, the Markov model introduced is capable of modeling molecular propagation in these two regions. However, the model should be revised. We explain the necessary modifications and then, put the propagation models for the three regions together in one Markov chain and solve it for stationary

probability distributions.

We start with defining states of the Markov chain. Assume x and y components of the propagation are independent. Here we build a Markov chain for the x component. Spatial steps are states of the Markov chain. In order to make a meaningful Markov chain, we consider the desired region as level 0, and the transient region as level 1. If Δx is a small enough spatial step and L is length of the desired region, level 0 of the Markov chain consists of $M = \left[\frac{L}{\Delta x}\right]$ states. Similarly, level 1 of the Markov chain consists of $N = \left[\frac{2d_{nn}}{\Delta x}\right]$ states. To have a consistent design, we consider levels $2, 3, ...$ (undesired region) have N states, too.

Having defined the Markov chain, transition probabilities should be derived. To do so, one needs jump sizes distribution and inter-jump distributions. Since the nano-relays used in the transient and undesired regions are similar, jump sizes in both regions have the same distribution. Assuming the oriented filament is exactly pointed towards the desired region, jump sizes distribution is calculated in Section 3.4.

Assuming oriented filaments are exactly directed towards the desire region might not be a realistic assumption. As mentioned earlier, if the filament oriented towards the desired region does not have any deviations, the probability distribution of the second part of the jump, J, is simply:

$$P(J = k\Delta x) = \begin{cases} 1 & k = L_d \\ 0 & k \neq L_d, \end{cases} \tag{3.54}$$

where $L_d = \left[\frac{L_m}{\Delta x}\right]$, and L_m is length of filaments. However, filaments directed towards the desired region might have deviations. We assume the specific filaments might be deviated from the x axis up to $\frac{\pi}{3}$, and have a uniform distribution in between. Looking at Figure 3.11, the jump size probability distribution for the second part is:

$$P(J = k\Delta x) = \begin{cases} \frac{\theta_k - \theta_{k+1}}{\frac{\pi}{3}} & k \leq L_{dd} \\ 0 & k > L_{dd}, \end{cases} \tag{3.55}$$

where,

$$\theta_k = acos((k\Delta x + \frac{\Delta x}{2})/L_m), \tag{3.56}$$

and $L_{dd} = \left[\frac{L_m}{2\Delta x}\right]$. The overall distribution will be convolution of the first part, derived in Section 3.4, and (3.55).

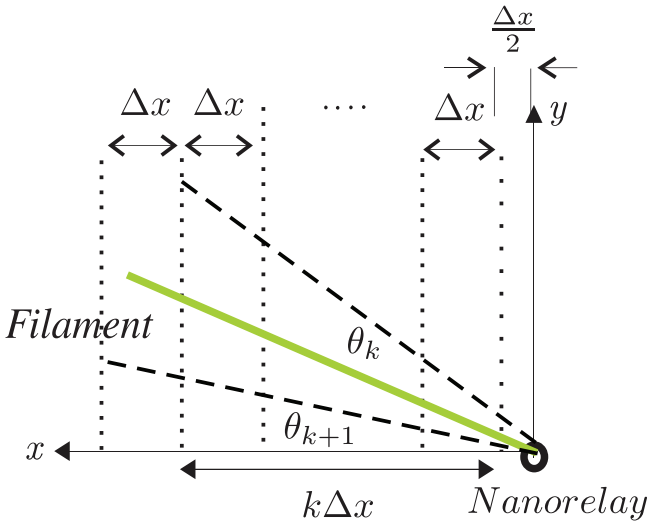

Figure 3.11: Second part of a jump, for jump size of $k\Delta x$.

As in Section 3.4, it is assumed inter-jump random variable has an exponential distribution. Also, the rate of the inter-jump random variable for molecular propagation in the undesired region is derived in Section 3.4. However, since the number of neighbors for nano-relays in the transient region and undesired region are not equal, the inter-jump rate in the transient region should be examined carefully. As mentioned before, in the considered scenario a motor detached from a filament belonging to an arbitrary nano-relay, called A, attaches to a filament belonging to the first, second, or third layers of A's neighbors. Consider the arbitrary node A in the transient region. Based on Figure 3.3, it is straightforward to show that there are average of 8 nano-relays in the first three layers of neighbors of A, if A is at most d_{nn} meters away from the boundary of the desired region (since there are no nano-relays in the desired region), and there are average of 11 nano-relays if A is between d_{nn} and $2d_{nn}$ meters away from the boundary. However, this number is 12 for a nano-relay in the undesired region. Now, consider λ as the inter-jump rate in the undesired region. So, the probability that a free molecule in the undesired region attaches to a filament in one time step is $\lambda\Delta t$. Therefore, attaching probability for a molecule detached from a nano-relay at most d_{nn} meters away from the boundary is $\frac{8}{12}\lambda\Delta t$,

and for a molecule detached from a nano-relay between d_{nn} and $2d_{nn}$ meters away from the boundary, attaching probability is $\frac{11}{12}\lambda\Delta t$. Consequently, the modified inter-jump rates are $\frac{8}{12}\lambda$ and $\frac{11}{12}\lambda$, respectively.

Having calculated all necessary distributions, we build the transition matrix. The first M rows of the transition matrix are filled based on (3.20), with the assumption that the boundaries are absorbing (considering Figure 3.10, molecules hitting the boundary can only move to the right). To fill the rest of the rows, (3.28) is used. For the next $\frac{N}{2}$ rows (states at most d_{nn} meters away from the boundary), $\lambda_a = \frac{8}{12}\lambda$, and $J_a \equiv J$. Next $\frac{N}{2}$ rows (states at between d_{nn} to $2d_{nn}$ meters away from the boundary) are filled with the assumption of $\lambda_a = \frac{11}{12}\lambda$, and $J_a \equiv J$, and finally, for the rest of the rows $\lambda_a = \lambda$ and $J_a \equiv J$. We should note that since the probabilities in (3.20) vanish quickly, and also considering the assumption that filaments are not longer than the average distance between nano-relays, transitions in the Markov chain are just one level up, or down. If either of these statements were not valid, we should have defined levels of the Markov chain in another way, to identify the matrix analytic behavior. Considering the above discussions, the transition matrix structure will be:

$$P = \begin{bmatrix} B & C & & & & \\ D & E & F & & & \\ & A_2 & A_1 & A_0 & & \\ & & A_2 & A_1 & A_0 & \\ & & & \ddots & \ddots & \ddots \end{bmatrix}. \tag{3.57}$$

Here, we consider matrix B and discuss derivation of its entries. Deriving other sub-matrices is similar. Assuming the desired region is longer than maximum step size of a molecule under Brownian motion (otherwise, the scenario will not be reasonable), B is shown in (3.58).

Since B represents molecular movement in the desired region, which is based on Brownian motion, the transition probabilities are derived based on (3.20). We explain two of them here, the rest can be derived similarly. b_i represents the probability that a molecule at state i ($i\Delta x$ meters away from the boundary) moves to the boundary (state 0) in the next time step. Since the boundary is on the left of the current position of the molecule, the movement should take place to the left. Also, considering an absorbing boundary, if the molecule moves more than $i\Delta x$ in Δt, it will be at the boundary in the next time step. Based on the above discussion, b_i is derived

$$
B = \begin{bmatrix}
b_0 & c_1 & \dots & c_m & & & & & & & & \\
b_1 & c_0 & c_1 & \dots & c_m & & & & & & & \\
\vdots & \vdots & \ddots & \ddots & \ddots & \ddots & & & & & & \\
b_{m-1} & \dots & c_{-1} & c_0 & c_1 & \dots & c_m & & & & & \\
c_{-m} & \cdots & c_{-2} & c_{-1} & c_0 & c_1 & \dots & c_m & & & & \\
 & c_{-m} & \cdots & c_{-2} & c_{-1} & c_0 & c_1 & \dots & c_m & & & \\
 & & \ddots & \ddots & \ddots & \ddots & \ddots & \ddots & \ddots & \ddots & & \\
 & & & c_{-m} & \dots & c_{-2} & c_{-1} & c_0 & c_1 & \dots & c_m & \\
 & & & & c_{-m} & \dots & c_{-2} & c_{-1} & c_0 & c_1 & \dots & c_m \\
 & & & & & c_{-m} & \dots & c_{-2} & c_{-1} & c_0 & \dots & c_{m-1} \\
 & & & & & & \ddots & \ddots & \ddots & \ddots & \ddots & \vdots \\
 & & & & & & & & c_{-m} & \cdots & c_{-1} & c_0
\end{bmatrix}. \tag{3.58}
$$

as:

$$
b_i = \sum_{j=-m}^{i} P(\tilde{X} = j\Delta x), \tag{3.59}
$$

where, $\tilde{X}$ is the step size for a molecule under Brownian motion and m is the maximum step size (it is assumed that the probability that a particle under Brownian motion moves for more than m states in Δt, is too small). Additionally, c_k represents probability of moving from state i (position of $i\Delta x$) to state $i+k$ (position of $(i+k)\Delta x$) in one time step, where neither of the states are boundary states. Therefore, it is straightforward to check $c_k = P(\tilde{X} = k\Delta x)$. Also, we note that if a molecule in one of the states $M - m$ to M moves longer than $(M - S)\Delta x$ in one time step, where S is the current state, the molecule moves to the transient region. Probabilities of such events are represented in matrix C. The remaining block matrices D, E, F, A_0, A_1, and A_2 can be obtained using (3.28).

To solve the Markov chain, consider x_i as the stationary probability distribution of level i. Defining matrix R as the minimal solution of the equation:

$$
R = A_0 + RA_1 + R^2 A_2, \tag{3.60}
$$

the stationary probability distribution will be derived solving the following equations:

$$[x_0\ x_1\ x_2]\begin{bmatrix} B & C & \\ D & E & F \\ & A_2 & A_1+RA_2 \end{bmatrix} = [x_0\ x_1\ x_2], \tag{3.61}$$

$$x_0\mathbf{e}_M + x_1\mathbf{e}_N + x_2(I-R)^{-1}\mathbf{e}_N = 1, \tag{3.62}$$

$$x_i = x_{i-1}R,\ i = 3,4,..., \tag{3.63}$$

where $\mathbf{e}_i$ is a column of length i, with ones as entries.

The main purpose of this chapter was analyzing molecular propagation in molecular communication using filaments and nano-relays. We started by introducing Brownian motion (Section 3.1), jump diffusion process (Section 3.2), and approximations for them (Section 3.3) as the tools that we needed to use to mathematically model the propagation. Next, we proposed a model and solved it for transient solution in Section 3.4. The stationary solution was then calculated in Section 3.5. The solutions for the model will be used in the next chapter to investigate performance of this type of molecular communication and derive the results.

Chapter 4

Results

4.1 Propagation in molecular communication using filaments

In this section, we use the proposed model to investigate the performance of the channel in terms of delay and error probability. First, we validate the model by comparing the analytic and simulation results. We find the propagation delay distribution function for two different settings of the channel based on the model and simulations, and show that the two sets of results match. Simulations are performed in MatLab. It is worth mentioning that in the simulations the transmitter releases a motor at time zero. Brownian motion is used to find dislocation of the motor before it reaches a filament. As time goes on, it is checked whether the motor has reached a filament. If yes, instead of Brownian motion, a movement with fixed speed with the direction of the filament is assumed for the motor until it reaches the nano-relay. Then, the movement will also be with fixed speed, directly towards the closest receiver (since the nano-relay puts the motor on the filament oriented towards the closest receiver). Upon reaching the end of the filament, the motor will start diffusing again. This goes on until the motor reaches one of the receivers. It is worth mentioning that it is assumed there are enough ATP molecules in the medium and if a motor hits a filament it will attach to the filament. Also, it is assumed motors do not detach from filaments unless they reach the end of the filament.

The channel in Figure 3.1 with dimensions of $50\mu m \times 50\mu m$ is considered for simulations. The values assigned to parameters for the simulations are as

follows. The diffusion coefficient is $1.0982 \times 10^{-12} m^2/s$. The average speed of motors moving on filaments is $10\mu m/s$. We consider two settings for the channel and show that the model can track the changes. As the first scenario, the rate of the Poisson point process is 10×10^9 $1/m^2$ (average of *25* nano-relays in the channel), the number of filaments attached to each nano-relay is *4*, and the lengths of the filaments are $10\mu m$. We explain reasoning for picking these values. As for the diffusion coefficient, we have:

$$D = (1/f)KT, \tag{4.1}$$

where, K is Boltzmann constant, T is absolute temperature, and f is derived as:

$$f = 6\pi hr, \tag{4.2}$$

where, h is the viscosity of the medium and r is the radius of the particle in the medium. In this thesis, we assumed $h = 0.001$ and $r = 200nm$. The value of h is close to blood viscosity, and r (radius of a motor and the molecule attached to it) is assumed to be $200nm$ (typical length of Kinesin is $80nm$; Figure 9.15 in [29]). Regarding the speed of molecular motors, the speed of Kinesins is between 0.02 to $2\mu m/s$, and speed of Myosins is between .2 to $60\mu m/s$ (Chapter 16, Molecular Motors Section, Motor Protein Kinetics Are Adapted to Cell Functions Subsection in [51]). Since we are considering both types of motors in the model, we picked $10\mu m/s$.

Figure 4.1(a) shows the comparison between analytic and simulation results for the scenario. As it is shown in Figure 4.1(a), the analytic and simulation results are in good match. Also, we included the results for the diffusion process (in this setting, there are no nano-relays, and a released information molecule diffuses through the medium until it reaches one of the receivers). We include this setting as a reference.

In the second scenario, the rate of the Poisson point process is 6×10^9 $1/m^2$ (average of *15* nano-relays in the channel), the number of filaments attached to each nano-relay is *6* and the length of them is $7\mu m$. We changed all the parameters. Figure 4.1(b) shows the comparison between the analytic and simulation results. The model tracks the performance of the channel well. The presented results validate the model and imply that jump diffusion process is capable of modeling the molecular propagation in molecular communication via filaments using nano-relays. In the following results, the setting of the channel is as follows, unless it is stated otherwise: the rate of the Poisson point process is 8×10^9 $1/m^2$ (average of *20* nano-relays in the

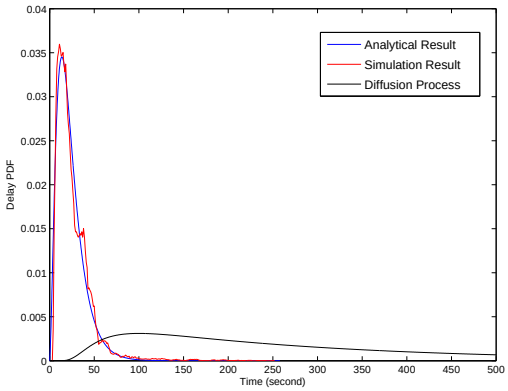

(a) Rate of Poisson point process is 10×10^9 $1/m^2$, *4* filaments attached to each nano-relay, with length $10\mu m$.

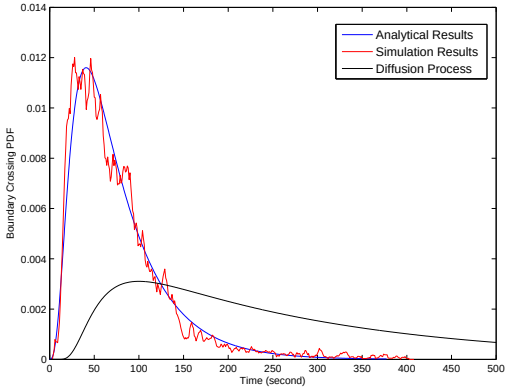

(b) Rate of Poisson point process is 6×10^9 $1/m^2$, *6* filaments attached to each nano-relay, with length $7\mu m$.

Figure 4.1: Analytical results vs. simulation results.

channel), the number of filaments attached to each nano-relay is *4*, and the length of them is $10\mu m$.

Figures 4.2, 4.3, and 4.4 show the delay performance of the channel. Figure 4.2 represent the delay of the channel if filaments with different length are used. If longer filaments are deployed in the channel, not only the prob-

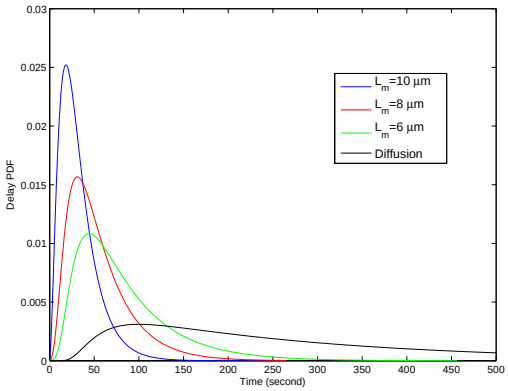

Figure 4.2: Delay probability distribution for different length of filaments.

ability that a diffusing motor attaches to any of them will increase, but also an attached motor will be guided towards a receiver for a longer distance. Therefore, increasing the length of the filaments will decrease the delay of the channel.

Figure 4.3 illustrates performance of the channel in terms of the delay for different number of filaments attached to each nano-relay. The probability that a motor attaches to a filament will increase if the number of filaments attached to a nano-relay increases, which will result in higher probability of guiding motors towards a receiver, and decreasing the delay.

Finally, Figure 4.4 shows the delay for two spatial rates of the nano-relays distribution. As shown in the figure, increasing number of the nano-relays in the channel enhances the performance of the channel in terms of the delay by increasing the probability that a motor attaches to a filament.

The bit error probability is an important issue in communication. We investigate this issue in molecular communication via filaments using nano-relays. For the channel in Figure 3.1, a specific modulation is considered and the average bit error probability is derived. The same approach could be used to find bit error probability of different modulation techniques. We assume the transmitter releases one information molecule attached to a motor as bit 1, and does not release any molecule as bit 0. Considering T_{inter} as the inter-symbol duration, we assume a released molecule is received at most $2T_{inter}$ after its release. Of course, if it is not received in T_{inter} seconds, an error may

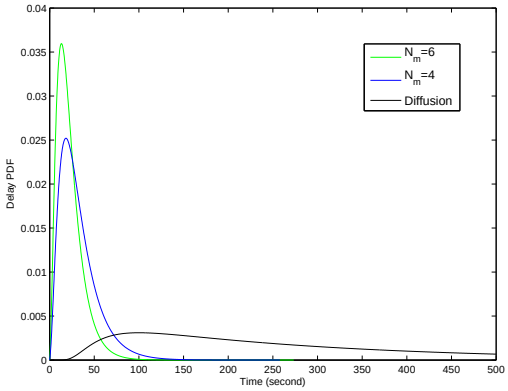

Figure 4.3: Delay probability distribution for different number of filaments attached to nano-relays.

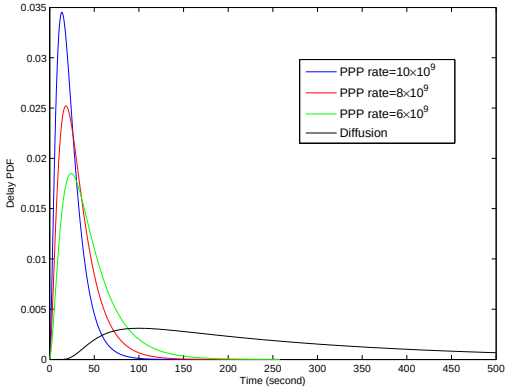

Figure 4.4: Delay probability distribution for different rate for Poisson point process.

Delay probability distribution for different rate for Poisson point process.

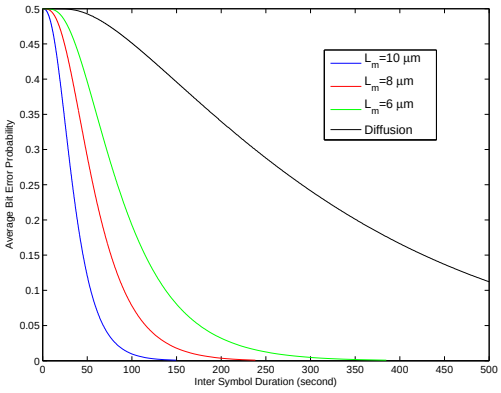

Figure 4.5: Average error probability distribution for different length of filaments.

happen. In other words, we assume inter-symbol interference is caused only by the last transmitted signal. This can be justified by assuming molecular messages dissolve in the channel after $2T_{inter}$ seconds. For this modulation technique, the average bit error probability is:

$$p_{error} = p_{error|1}p(1) + p_{error|0}p(0), \tag{4.3}$$

where, $p(0)$ is probability of sending bit 0, $p(1)$ is probability of sending bit 1, and:

$$p_{error|1} = p(0)p_{int} + p(1)(1 - p_{int})p_{int}, \tag{4.4}$$

$$p_{error|0} = p(1)p_{int}, \tag{4.5}$$

where, p_{int} is the probability that a released molecule does not reach either of the receivers in T_{inter} seconds. Assuming $p(0) = p(1) = \frac{1}{2}$, and finding p_{int} from propagation delay distribution function, we derive the error probability. We note that since nano-relays do not decode messages and only put the arrived molecule on the filament oriented towards the closest receiver, no error is generated by nano-relays.

Figures 4.5, 4.6, and 4.7 show average error probability versus inter-symbol duration. Figure 4.5 illustrates the effect of the length of filaments on the average bit error probability, Figure 4.6 shows the error probability as a function of the number of filaments attached to a nano-relay, and Figure

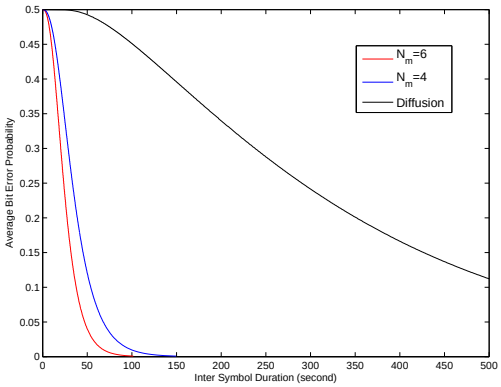

Figure 4.6: Average error probability distribution for different number of filaments attached to nano-relays.

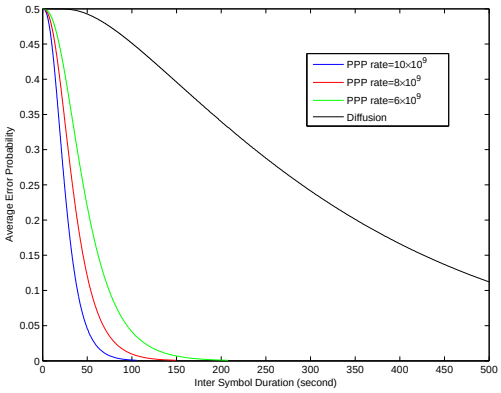

Figure 4.7: Average error probability distribution for different rate for Poisson point process.

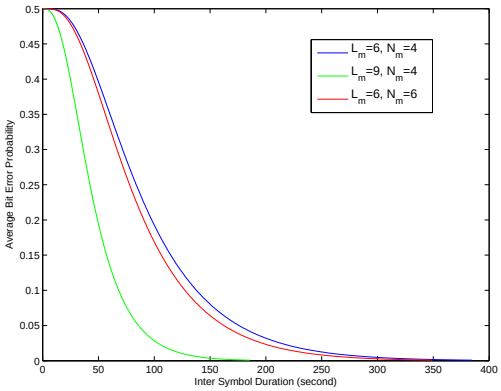

Figure 4.8: Comparing the effect of the length and the number of attached filaments attached to each nano-relays in terms of average bit error probability.

4.7 illustrates error probability for different spatial rates of nano-relays. In all cases, a similar discussion as was presented for delay distribution can be done to elaborate on the reason for performance improvements.

As the last set of results, we investigate the trade off between increasing the length of filaments or the number of filaments attached to nano-relays. Assume 4 filaments with length of $6\mu m$ are already attached to each nano-relay. We assume there are enough tubulins for each nano-relay to grow $12\mu m$ of filaments (tubulins are a kind of proteins, which are building blocks of filaments). The question is which one is better in terms of average bit error probability: growing two new filaments with length of $6\mu m$, or growing current filaments for $9\mu m$? Figure 4.8 shows the average bit error probability for both improvements. As expected, both decisions reduce error probability. However, growing the current filaments is more beneficial for improving the average bit error probability.

Now we analyze the steady state performance of the system. In the following results, the setting of the channel is as follows unless it is stated otherwise: the length of the desired region in $50\mu m$, the diffusion coefficient is $1.0982 \times 10^{12} m^2/s$, the average speed of motors walking on filaments is $10\mu m/s$, the rate of the Poisson point process is $8 \times 10^9 m^{-2}$ (average of 20

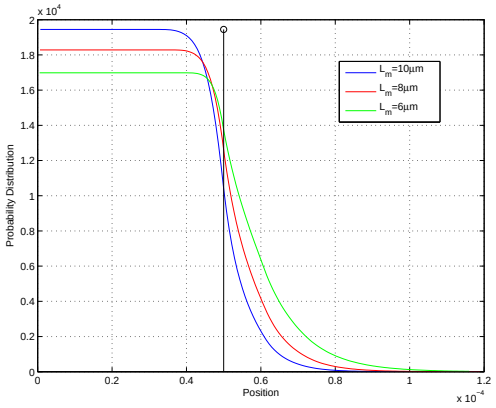

Figure 4.9: Stationary probability distribution for position of a molecule for different lengths of filaments.

nano-relays in an area of $50\mu m \times 50\mu m$), and 4 filaments, each $10\mu m$ long, are attached to all nano-relays.

As the first set of results, Figure 4.9 shows stationary probability distribution for position of a molecule in the discussed scenario for different lengths of filaments attached to nano-relays. The black line shows the boundary of the desired region. As illustrated in the figure, increasing length of filaments will increase chance of keeping a molecule in the desired region. Increasing the lengths of filaments increases the probability that a free molecule attaches to a filament, and also increases the jump sizes. Both will lead to higher probability for staying at the desire region. Also, as filaments grow longer, they will enter the desired region more. This causes the probability distribution to start to bend from stats farther to the boundary of the desired region.

Figure 4.10 shows the next set of results. It illustrates the effect of Poisson point process, based on which nano-relays are distributed in the transient and undesired region, on the stationary probability distribution. Increasing the rate of the process will increase the average number of nano-relays which will increase the probability that a molecule attaches to a filament.

Next set of results answers the question of "more filaments or longer filaments?" in the steady state scenario. We assume four $6\mu m$ long filaments are already attached to nano-relays. Consider two scenarios: each nano-relay grows filaments to $9\mu m$, or each nano-relay adds two more filaments

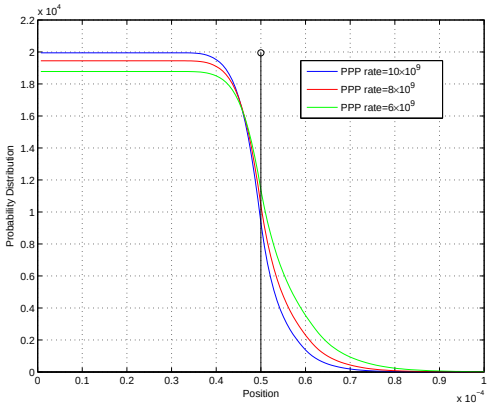

Figure 4.10: Stationary probability distribution for position of a molecule for different rates for Poisson point process.

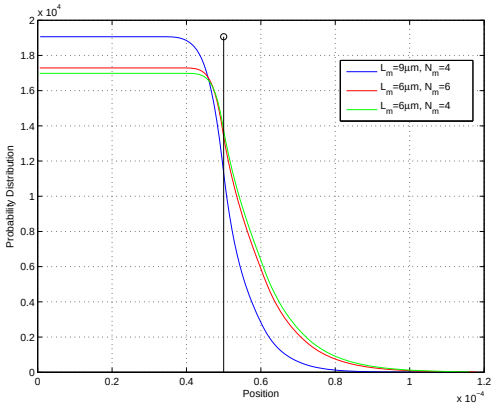

Figure 4.11: Longer filaments or more filaments?

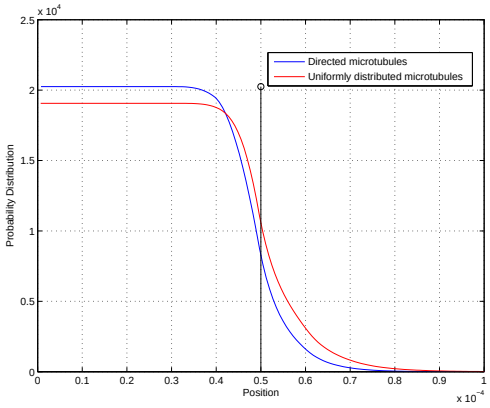

Figure 4.12: How important directed filaments are?

each $6\mu m$ long. The two scenarios are chosen in a way that the amount of needed resources are equal. Based on Figure 4.11, length of filaments affects performance of the system more efficiently and is more advantageous compared with increasing the number of filaments attached to nano-relays. It can be justified by considering that adding more filaments increases the probability that a motor attaches to them. However, increasing the length of filaments not only increases the probability of attachment, but also increases the jumps sizes.

The last set of results illustrates inefficiency caused by deviation of directed filaments. We consider the default configurations for the channel, but two settings for directed filaments: directed filaments are exactly set to point to the undesired region, and are uniformly distributed on the left side of nano-relays. Figure 4.12 shows the stationary probability distribution for molecules in the two settings. As illustrated in the figure, as long as the specific filament directs molecules towards the desired region, no matter how much, final probability distribution of the position of molecules is concentrated at the desired region.

Chapter 5

Conclusion and Recommendations

Molecular communication is a promising bio-inspired solution for communications in nano-networks. In this thesis, first we investigated three molecular communication methods: diffusion, molecular communication using physical contact, and molecular communication via filaments. Starting with diffusion, we discussed several proposed modulation techniques. Then, in a more detailed study, we presented a literature review on the molecular communication via physical contact. We divided this method into two subcategories and investigated each by reviewing the research work that has been done on them. The last molecular communication method introduced in this thesis was communication via filaments. We presented a simulation technique, and two common scenarios considered in the literature.

In communication via filaments, a transmitter releases information molecules which are bound to specific molecules known as molecular motors. Molecular motors can attach to filaments, and move along them, while carrying information molecules, to reach at the receiver. The most realistic scenario in the literature for communication using filaments is communication in free space. In this scenario, it is assumed that a number of filaments are attached to receivers. A released information molecule diffuses through the medium and in case it reaches a filament it will attach to the filament, and moves along it to get to the receiver. This scenario showed a poor performance in terms of the coverage range and delay. We proposed relay nano-machines employment as a technique to overcome these drawbacks, and used jump diffusion process to model molecules propagation in this scenario. Unfortunately, jump

diffusion process is not developed thoroughly. Therefore, we approximated this process using a discrete time Markov chain and used Markov chains to model propagation process.

In the next step, we modified the model to analyze steady state behavior of the system. We presented a new scenario and discussed necessary modifications for the model. Also, we relaxed the assumption of oriented filaments, which makes the model more realistic. We showed in Section 4 that the proposed scenario is capable of keeping information molecules in a desired region.

Before using our model to investigate molecular communication via filaments using nano-relays, the analytic model was validated by comparing results with simulation results. It was shown for two completely different scenarios that the results from the model match those from simulations.

We used the model to capture the delay of a transmitted molecule and show its advantage over free diffusion, as a reference. Comparing this set of results with those found for free diffusion showed that using relay nanomachines leads to reducing the delay of a nano-network, resulting in performance enhancements. We also investigated the effect of different parameters in delay performance of the system.

The last set of results investigated steady state performance of the system. First, it was shown that the proposed scenario is capable of keeping information molecules in a desired region. This can be very helpful in drug delivery systems. We also investigated the effect of different parameters in performance of the system. Finally, we presented a set of results which illustrates the importance of the accuracy of the orientation. The performance of the system is compared between the two scenarios where the orientation is ideal and the directed filament is uniformly distributed between $-\frac{\pi}{3}$ and $\frac{\pi}{3}$ with respect to the closest receiver. Based on the results in this thesis, there is not much difference between these two scenarios. This can be explained considering that it is presented for the steady state of the system.

Generally, molecular communication methods lack speed and are not capable of directional communication. For example, diffusion which is the most common technique has both of the mentioned drawbacks. Employing nano-relays, which was proposed in this research work, can be used to overcome these drawbacks. Nano-relays are capable of improving performance of the system if they are implemented in an efficient way. As mentioned before, there has been some research addressing this issue for molecular communication via diffusion. However, other types of molecular communication need

to be investigated to see if implementing nano-relays can improve the performance of the method. We would like to note that using nano-relays means using more resources such as nano-machines, and in our case more filaments. We assumed there is an unlimited access to resources, which might not be true for some applications. Therefore, depending on the application it might be necessary to investigate the trade off between improving the performance and using resources.

The model proposed in this thesis is based on simple biological assumptions. We note that some biological assumptions can be modified to make the model more accurate. For instance, since our focus was on finding the propagation model we assumed that the structure of filaments is a thin line. However, filaments have complicated structures, which can affect the performance of the model. The effects could be in the probability that a motor attaches to a filament, direction of the filament, etc.

Several molecular communication techniques, such as molecular communication using diffusion, bacteria, and hybrids of them with other methods, are modeled using Brownian motion. Since the equations describing Brownian motion are complicated, it is not straightforward to model complicated scenarios and therefore, most research consider simple scenarios. However, the approach proposed in this thesis makes it easy to consider complicated scenarios. The idea was to assume that the space is discrete, which makes deriving complicated distributions straightforward. For example, Wei *et al.* [55] propose an analytic model for molecular communication using bacteria. They propose a continuous space Markov chain to model movement of bacteria and present the equations. The model they propose is not an approximation. However, the model consists of several equilibrium equations and solving the model is complicated. Considering a discrete space, the model becomes a set of probabilities in a transition matrix. We note that the drawback for the method used in this thesis is the size of the Markov chain. If the size of the scenario becomes large or a very low error is needed, the size of the Markov chain becomes huge and generally, solving it is not straightforward.

One of the issues with molecular communication using diffusion is that movement of the molecules is random and targeted communication is not feasible. However, there is a scenario based on what is proposed in this thesis that the author believes it is worth investigating to overcome this issue. Assume there is one central transmitter and several filaments are attached to the transmitter. Each filament is oriented towards a nano-machine and

is long enough to get close to the nano-machine. If the transmitter uses the filaments to communicate with the nano-machines, when a motor reaches the end of the filament it starts diffusing. The distance the motor should diffuse to reach the nano-machine is short. It makes the receiving probability high. The central transmitter could be more complicated than other nano-machines, and can communicate with other central transmitters using more complicated methods. This technique is similar to cellular communication. The approximation method discussed in this thesis is an appropriate candidate to analyze this system. Finally, since the model proposed in this thesis is straightforward to be implemented, the author is hoping the model will be useful in analyzing systems going to be implemented.

Bibliography

[1] N. R. Lacasa, *Modeling the Molecular Communication Nanonetworks*, Georgia Institute of Technology, 2009.

[2] J. E. Hall, *Guyton and Hall textbook of medical physiology*, Elsevier Health Sciences, 2015.

[3] C. Veigel and C. F. Schmidt, "Moving into the cell: Single-molecule studies of molecular motors in complex environments," *Nature Reviews Molecular Cell Biology*, vol. 12, pp. 163–176, March 2011.

[4] I. Akyildiz, F. Brunetti, and C. Blazquez, "Nanonetworks: A new communication paradigm," *Computer Networks*, vol. 52, pp. 2260–2279, Aug 2008.

[5] B. Atakan and O. B. Akan, "Carbon nanotube-based nanoscale ad hoc networks," *IEEE Communications Magazine*, vol. 48, pp. 129–135, June 2010.

[6] T. Bacinoglu, B. Gulbahar, and O. B. Akan, "Constant fidelity entanglement flow in quantum communication networks," *in Proc. CLOBECOM*, pp. 1–5, Dec 2010.

[7] M. Kuscu and O. B. Akan, "A nanoscale communication channel with fluorescence resonance energy transfer (fret)," *in Proc. INFOCOM*, pp. 425–430, April 2011.

[8] T. Nakano, M. J. Moore, F. Wei, A. V. Vasilakos, and J. Shuai, "Molecular communication and networking: opportunities and challenges," *IEEE Transactions on Nanobioscience*, vol. 11, pp. 135–148, June 2012.

[9] M. Kuran, H. B. Yilmaz, T. Tugcu, and B. Ozerman, "Energy model for communication via diffusion in nanonetworks," *Nano Comunication Networks*, vol. 1, pp. 86–95, June 2010.

[10] M. U. Mahfuz, D. Makrakis, and H. Mouftah, "Characterization of intersymbol interference in concentration-encoded unicast molecular communication," *in Proc. Canadian Conference on Electrical and Computer Engineering*, pp. 164–168, May 2011.

[11] M. J. Moore, A. Enomoto, T. Nakano, A. Kayasuga, H. Kojima, H. Sakakibara, K. Oiwa, and T. Suda, "Molecular communication: simulation of microtubule topology," *in Proc. Information and Communications Technology*, vol. 1, pp. 134–144, Dec 2006.

[12] H. C. Berg, *Random Walks in Biology*, Princeton University Press, 1993.

[13] I. Llatser, E. Alarc, and M. Pierobon, "Diffusion-based channel characterization in molecular nanonetworks," *in Proc. IEEE Conference on Computer Communications Workshops, INFOCOM Wksps*, pp. 467–472, April 2011.

[14] M. S. Kuran, H. B. Yilmaz, T. Tugcu, and Akyildiz. I. F., "Modulation techniques for communication via diffusion in nanonetworks," *in Proc. IEEE ICC*, June 2011.

[15] M. U. Mahfuz, D. Makrakis, and H. Mouftah, "Spatiotemporal distribution and modulation schemes for concentration encoded medium-to-long range molecular communication," *in Proc. 25th Biennial Symposium on Communications, Networking and Broadcasting*, pp. 100–105, May 2010.

[16] M. Pierobon and I. F. Akyildiz, "Information capacity of diffusion based molecular communication in nanonetworks," *in Proc. INFOCOM*, pp. 506–510, April 2011.

[17] M. Pierobon and I.F. Akyildiz, "Diffusion-based noise analysis for molecular communication in nanonetworks," *IEEE Transactions on Signal Processing*, vol. 59, pp. 2532–2547, June 2011.

[18] T. Nakano, T. Suda, T. Koujin, T. Haraguchi, and Y. Hiraoka, "Molecular communication through gap junction channels: System design, experiments and modeling," *in Proc. Bio-Inspired Models of Network, Information and Computing Systems*, pp. 139–146, Dec 2007.

[19] T. Nakano, T. Suda, M. Moore, R. Egashira, A. Enomoto, and K. Arima, "Molecular communication for nanomachines using intercellular calcium signaling," *in Proc. 5th IEEE Conference on Nanotechnology*, vol. 2, pp. 478–481, July 2005.

[20] T. Nakano and J. Shuai, "Repeater design and modeling for molecular communication network," *in Proc. INFOCOM*, pp. 501–506, April 2011.

[21] D. Kilinc and O. B. Akan, "An information theoretical analysis of nanoscale molecular gap junction communication channel between cardiomyocytes," *IEEE Transactions on Nanotechnology*, vol. 12, pp. 129–136, March 2013.

[22] T. Nakano, Y. Hsu, W. C. Tang, T. Suda, D. Lin, T. Koujin, T. Haraguchi, and Y. Hiraoka, "Microplatform for intercellular communication," *in Proc. 3rd IEEE Int. Conf. on Nano/Micro Engineered and Molecular Systems*, pp. 476–479, Jan 2008.

[23] L. Galluccio, S. Palazzo, and G. Santagati, "Characterization of signal propagation in neuronal systems for nanomachine-to-neurons communications," *in Proc. IEEE Conference on Computer Communications Workshops (INFOCOM WKSHPS)*, pp. 437–442, April 2011.

[24] L. Galluccio, S. Palazzo, and G. E. Santagati, "Modeling signal propagation in nanomachine-to-neuron communications," *Nano Communication Networks*, vol. 2, pp. 213–222, Dec 2011.

[25] E. Balevi, *A physical channel model and analysis of nano-scale neurospike communication*, Middle East Technical University, Aug 2010.

[26] A. Guney, B. Atakan, and O. B. Akan, "Mobile ad hoc nanonetworks with collision-based molecular communication," *IEEE Transactions on Mobile Computing*, vol. 11, pp. 353–366, March 2012.

[27] A. Vahdat and D. Becker, "Epidemic routing for partially-connected ad hoc networks," *technical report, Duke Univ.*, 2000.

[28] S. Balasubramaniama, N. Boyle, A. Della-Chiesa, F. Walsha, A. Mardinoglu, D. Botvich, and A. Prina-Mello, "Development of artificial neuronal networks for molecular communication," *Nano Communication Networks*, vol. 2, pp. 150–160, Sept 2011.

[29] G. Karp, "Cell and molecular biology; concepts and experiments," 2013.

[30] M. Moore, A. Enomoto, T. Nakano, R. Egashira, T. Suda, A. Kayasuga, H. Kojima, H. Sakakibara, and K. Oiwa, "A design of a molecular communication system for nanomachines using molecular motors," *in Proc. 4th Annual IEEE International Conference on Pervasive Computing and Communications*, pp. 559–565, March 2006.

[31] A. Enomoto, M. Moore, T. Nakano, R. Egashira, T. Suda, A. Kayasuga, H. Kojima, H. Sakakibara, and K. Oiwa, "A molecular communication system using a network of cytoskeletal filaments," *in Proc. NSTI Nanotechnology Conference and Trade Show*, vol. 1, pp. 725–728, 2006.

[32] N. Farsad, A. W. Eckford, and S. Hiyama, "Channel design and optimization of active transport molecular communication," *in Proc. International Conference on Bio-Inspired Models of Network, Information, and Computing Systems*, pp. 213–223, Dec 2011.

[33] S. F. Bush and S. Goel, "Persistence length as a metric for modeling and simulation of nanoscale communication networks," *in IEEE Journal on Selected Areas in Communications/Supplement*, vol. 31, pp. 815–824, Dec 2013.

[34] A. W. Eckford, N. Farsad, S. Hiyama, and Y. Moritani, "Microchannel molecular communication with nanoscale carriers: brownian motion versus active transport," *in Proc. 10th IEEE Conference on Nanotechnology*, pp. 854–858, Aug 2010.

[35] L. C. G. Rogers and D. Williams, *Diffusions, Markov Processes, and Martingales*, Cambridge University press, Cambridge, UK, 2000.

[36] N. Farsad, A. W. Eckford, S. Hiyama, and Y. Moritani, "Information rates of active propagation in microchannel molecular communication," *in Proc. International Conference on Bio-Inspired Models of Network, Information, and Computing Systems*, pp. 16–21, Dec 2010.

[37] A. W. Farsad, N.and Eckford, S. Hiyama, and Y. Moritani, "A simple mathematical model for information rate of active transport molecular communication," *in Proc. IEEE INFOCOM, Computer Communications Workshop*, pp. 473–478, April 2011.

[38] N. Farsad, A. W. Eckford, and S. Hiyama, "A mathematical channel optimization formula for active transport molecular communication," *in Proc. ICC*, pp. 6137–6141, June 2012.

[39] A. W. Eckford N. Farsad and S. Hiyama, "Design and optimizing of on-chip kinesin substrates for molecular communication," *in IEEE Transactions on Nanotechnology*, vol. 14, pp. 699–708, July 2015.

[40] N. Farsad, A. W. Eckford, S. Hiyama, and Y. Moritani, "Quick system design of vesicle-based active transport molecular communication by using a simple transport model," *Nano Communication Networks*, vol. 2, pp. 175–188, Dec 2011.

[41] M. J. Moore, A. Enomoto, T. Suda, A. Kayasuga, and K. Oiwa, "Molecular communication: uni-cast communication on a microtubule topology," *in Proc. IEEE International Conference on Systems, Man and Cybernetics*, pp. 18–23, Oct 2008.

[42] M. J. Moore, T. Suda, and K. Oiwa, "Molecular communication: modeling noise effects on information rate," *IEEE Transactions on Nanobioscience*, vol. 8, pp. 169–180, June 2009.

[43] M. J. Moore, A. Enomoto, S. Watanabe, K. Oiwa, and T. Suda, "Simulating molecular motor uni-cast information rate for molecular communication," *in Proc.l Conference on Information Sciences and Systems*, pp. 859–864, March 2009.

[44] S. Hiyama, R. Gojo, T. Shima, S. Takeuchi, and K. Sutoh, "Biomolecular-motor-based nano- or microscale particle translocations on dna microarrays," *Nano Letters*, vol. 9, pp. 2407–2413, April 2009.

[45] S. Hiyama, Y. Moritani, R. Gojo, S. Takeuchic, and K. Sutoh, "Biomolecular-motor-based autonomous delivery of lipid vesicles as nano- or microscale reactors on a chip," *Lap Chip*, vol. 10, pp. 2741–2748, Oct 2010.

[46] A. Enomotoa, M. J. Moorea, T. Suda, and K. Oiwab, "Design of self-organizing microtubule networks for molecular communication," *Nano Communication Networks*, vol. 2, pp. 16–24, March 2011.

[47] M. C. Tarhan, L. Jalabert, R. Yokokawa, C. Bottier, D. Collard, and H. Fujita, "Nano monorail for molecular motors: individually manipulated microtubules for kinesin motion," *in Proc. International Conference on Solid-State Sensors, Actuators and Microsystems*, pp. 2164–2167, June 2009.

[48] S. G. Kou and Hui Wang, "First passage time of a jump diffusion process," *Adv. Appl. Prob.*, vol. 35, pp. 504–531, 2003.

[49] N. Cai, "On first passage times of a hyper-exponential jump diffusion process," *Operations Research Letters*, vol. 37, pp. 127–134, March 2009.

[50] J. C. Fu and T. Wu, "Linear and nonlinear boundary crossing probabilities for brownian motion and related processes," *The J. Appl. Prob.*, vol. 47, 2010.

[51] B. Alberts, *Molecular Biology of the Cell*, Garland Science, 2008.

[52] G. E. Kreitzer Z. Mamdouh and W. A. Muller, "Leukocyte transmigration requires kinesin-mediated microtubule-dependent membrane trafficking from the lateral border recycling compartment," *The Journal of Experimental medicine*, vol. 205, pp. 951–966, 2008.

[53] A. Kamal and Lawrence S.B Goldstein, "Principles of cargo attachment to cytoplasmic motor proteins," *Current Opinion in Cell Biology*, vol. 14, pp. 63–68, 2002.

[54] G. Klein, "Mean first-passage times of brownian motion and related problems," *in Proc. of the Royal Society of London. Series A, Mathematical and Physical Sciences*, vol. 211, pp. 431–443, 1952.

[55] P. Bogdan GG. Wei and R. Marculescu, "Bumpy rides modeling the dynamics of chemotactic interacting bacteria," *IEEE Journal on Selected Areas in Communications*, vol. 31, pp. 879–890, Dec 2013.

Appendix

The list of abbreviations used in this thesis is as follows:

AM	amplitude modulation
BAC	binary asymmetric channel
CSK	concentration shift keying
DTMC	discrete time Markov chain
FM	frequency modulation
FSK	frequency shift keying
iid	dependent and identically distributed
ISI	inter-symbol interference
M-AM	multilevel amplitude modulation
MoSK	molecule shift keying
OOK	on-off keying
PPP	Poisson point process
SNR	signal to noise ratio